CHAPTER 3
RESULTS AND DISCUSSION

DEVELOPMENT AND EVALUATION OF THE YEAST BIOASSAY

3.1 DEVELOPMENT AND OPTIMISATION OF THE YEAST BIOASSAY

3.1.1 PHYSIOLOGICAL STUDIES OF THE INDUCTION OF β-GALACTOSIDASE IN *K. MARXIANUS*

Initial studies during the bioassay development examined the expression of β-galactosidase by *K. marxianus*. An adaptation of the method of Miller (1972) was used for the determination of β-galactosidase activity; the assay, which uses o-nitrophenyl-β-D-galactopyranoside (ONPG) as the chromogenic substrate was first optimised prior to use in the determination of the effect of carbon source and gratuitous inducers on the induction of β-galactosidase in *K. marxianus*.

3.1.1.1 Assessment and optimisation of the β-galactosidase (ONPG) assay

During an induction experiment, it is expected that the level of β-galactosidase activity will vary considerably, depending on the carbon source available to the yeast and the number of yeast cells present in the assay sample. The assay method was therefore assessed and optimised to allow the accurate determination of β-galactosidase activity at all stages in the growth cycle for all carbon sources and/or inducers used.

3.1.1.1.2 Effect of the cell density of assay samples on the determination of β-galactosidase activity

The effect of the cell denstiy of assay samples on the determination of β-galactosidase activity using ONPG was determined using lactose-grown cells at various stages in the growth cycle, as detailed in section 2.2.1.2.1. At each stage in the growth cycle, cells were diluted (see Table 35) prior to the determination of cell density (A_{620}) and the absorbance of the o-nitrophenol cleavage product of ONPG at 420nm (A_{420}). The data is shown in Table 35. These values were used to calculate the level of β-galactosidase activity (β-gal) in the original undiluted sample and these vaules are also shown in Table 35 The relationship between cell densitiy (A_{620}) and the absorbance of nitrophenol at 420nm (A_{420}) is shown in Figure 16.

Time	0 hours			2 hours		
Dilution	A_{620}	A_{420}	* β-gal	A_{620}	A_{420}	* β-gal
x10	0.04	0.230	217	0.070	0.590	323
x20	0.02	0.113	213	0.035	0.310	339
x50	0.008	0.049	231	0.014	0.121	331
x100	n.d.	n.d.	n.d.	0.004	0.053	290
x200	n.d.	n.d.	n.d.	n.d.	n.d.	n.d.

Time	4 hours			6 hours		
Dilution	A_{620}	A_{420}	* β-gal	A_{620}	A_{420}	* β-gal
x10	0.15	1.800	453	0.2	2.000	378
x20	0.075	1.200	604	0.1	1.500	566
x50	0.03	0.690	869	0.04	1.200	1133
x100	0.015	0.350	881	0.002	0.670	1266
x200	0.0075	0.169	851	0.001	0.345	1303

Table 35 Effect of cell densitiy (A_{620}) of assay samples on the determination of β-galactosidase activity using ONPG (A_{420}). Calculated levels of enzyme activity in undiluted samples (nmol/ml/min/A_{620}) are also shown (* β-gal). n.d. = not determined.

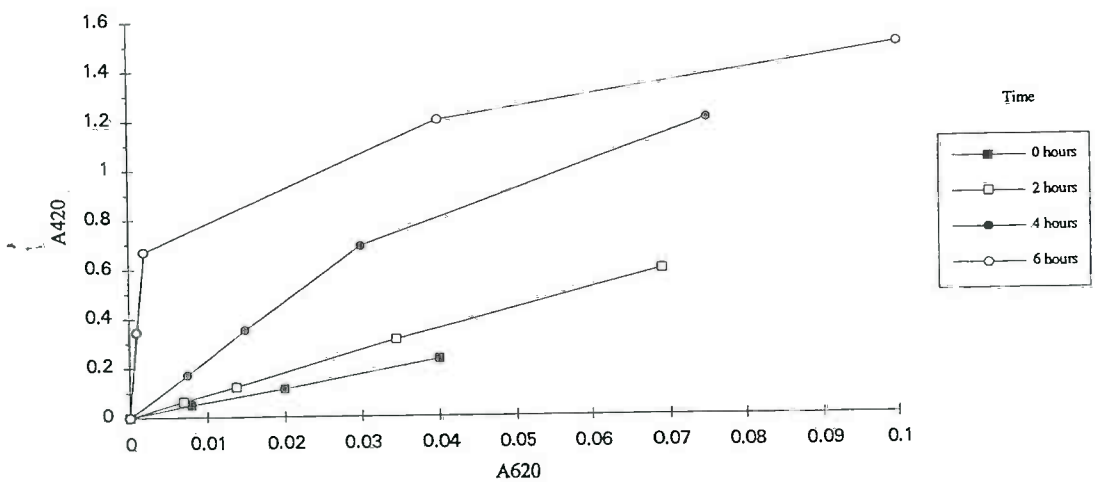

Figure 16 Relationship between cell densitiy of assay samples (A_{620}) and determination of β-galactosidase activity using the cleavage of ONPG (A_{420}) for lactose-grown cells at various stages in the growth cycle

At early stages in the growth cycle (0 and 2 hours) during which enzyme activity is low there was a linear relationship between A_{620} (cell density) and A_{420} (absorbance of the cleavage product at 420nm), (Figure 16), and it was therefore not necessary to dilute the samples by a greater factor than 10. At the later stages in the growth cycle the relationship between A_{620} and A_{420} was linear for only for samples with lower cell densities (100- and 200-fold dilutions) with the reaction being substrate limited at the higher cell densities (10-, 20- and 50- fold dilutions). The ONPG assay procedure includes a 10-fold dilution in the methodology (see section 2.2.1.1.4), and samples were therefore assayed from neat, with the exception of those taken from induced cultures (lactose- and galactsose-grown) after 4 hours of growth; these were diluted 10-fold prior to assaying, thereby giving a total of a 100-fold dilution.

3.1.1.1.2 Linearity of the cleavage of ONPG with respect to time..

The linearity of the cleavage of ONPG with respect to time by lactose- and glucose-grown cells at various stages in the growth cycle was assessed, as detailed in section 2.2.1.2.2. Representative progress curves for the cleavage of ONPG with respect to time are shown in Figure 17.

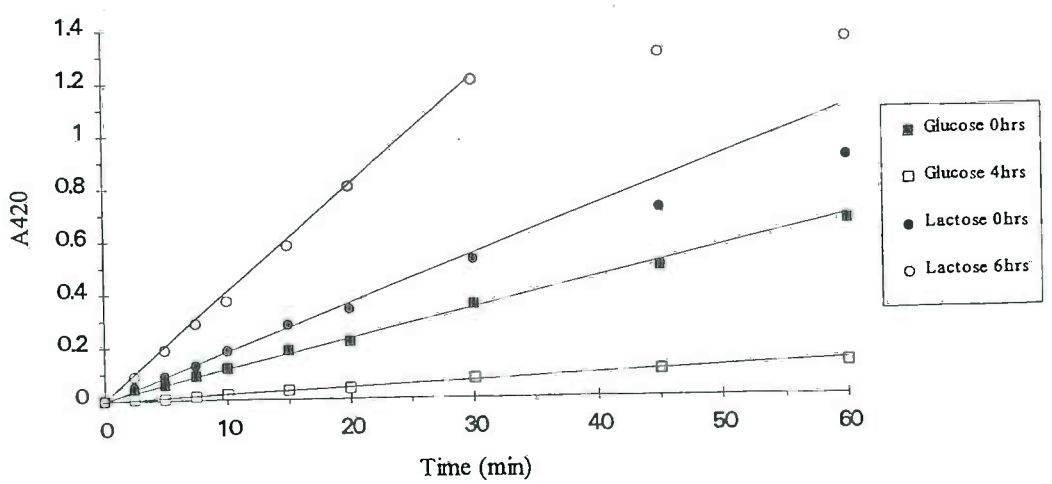

Figure 17 Time-dependent cleavage of ONPG by β-galactosidase from cells at various stages in the growth cycle.

For glucose-grown cells, in which enzyme activity was low throughout the growth cycle, the cleavage of ONPG was linear for up to one hour incubation at all stages in the growth cycle, whereas for lactose-grown cells, the cleavage of ONPG was linear only for up to 30 minutes incubation. Therefore, within these time limits the assay was not substrate-limited, and the assay was stopped (by the addition of sodium carbonate) at a known time, within these limits.

3.1.1.1.3 Effect of storage of samples at 4°C prior to assaying for β-galactosidase activity

The effect of storing samples in Z-buffer at 4°C prior to assaying for β-galactosidase activity was determined, as detailed in section 2.2.1.2.3. The absorbance of the o-nitrophenol cleavage product of ONPG at 420nm and the calculated level of β-galactosidase activity (β-gal activity) after various storage times are shown in Table 36.

Time (hrs)	A_{420}	* β-gal activity
0	0.55	281
0.5	0.58	296
1	0.53	271
2	0.52	266
3	0.59	301
4	0.55	281
5	0.52	266

* β-gal activity - β-galactosidase activity (nmol/ml/min/A_{620})

Table 36 Effect of storage of samples at 4°C on β-galactosidase activity

As can be seen from Table 36, β-galactosidase activity of samples was clearly not significantly affected by up to 5 hours storage at 4°C in Z-buffer and samples were routinely stored under such conditions until a sufficient number of samples were available for assaying.

These initial experiments established the assay conditions for the determination of β-galactosidase activity using ONPG, and were used in the induction experiments reported below.

To summarise, assay conditions were varied depending on the cell density of the sample and the carbon source used to supplement the media. Samples were diluted 10-fold prior to assaying for β-galactosidase activity, only when taken from induced cultures (lactose- or galactose-grown) after 2 hours of growth (see Table 22, page 67). Samples were incubated with ONPG for a varying, known, length of time, this being less than 30 minutes for samples from induced cultures (lactose- or galactose-grown) and less than 60 minutes for samples from uninduced (glucose-grown) cultures. All samples could be stored at 4°C until a sufficient number were available for assaying.

3.1.1.2 Effect of carbon source on growth and β-galactosidase activity of *K. marxianus*

The effect of five carbon sources on the growth rate and β-galactosidase activity of *K. marxianus* was determined as detailed in section 2.2.1.3.

Representative growth curves for *K. marxianus* on each carbon source are shown in Figure 18 and the effect of carbon source on β-galactosidase activity is shown in Figure 19.

As can be seen from Figure 18, *K. marxianus* grew fastest on glucose, lactose and galactose (doubling times being 84, 90 and 111 minutes, respectively), whereas growth rates on sorbitol and glycerol were considerable slower (165 and 186 minutes, respectively).

Glycerol and sorbitol had no detectable effect on the expression of β-galactosidase activity (Figure 19), which remained relatively constant throughout the growth cycle, at a level of approximately 150nmol/ml/min/A_{620}. Galactose and lactose both induced β-galactosidase activity, with maximal levels being reached around the onset of the stationary phase of growth (Figure 19); galactose induced slightly higher levels of activity than lactose, and activity, relative to sorbitol, was 6.73 and 9.29, respectively. In contrast, glucose repressed β-galactosidase activity during the lag and log phases of

growth. However enzyme activity was "derepressed" as stationary phase was entered, with final levels of activity being slightly higher than those for glycerol or sorbitol-grown cultures (Figure 19) and the activity, relative to sorbitol, was 1.83 for glucose-grown cultures.

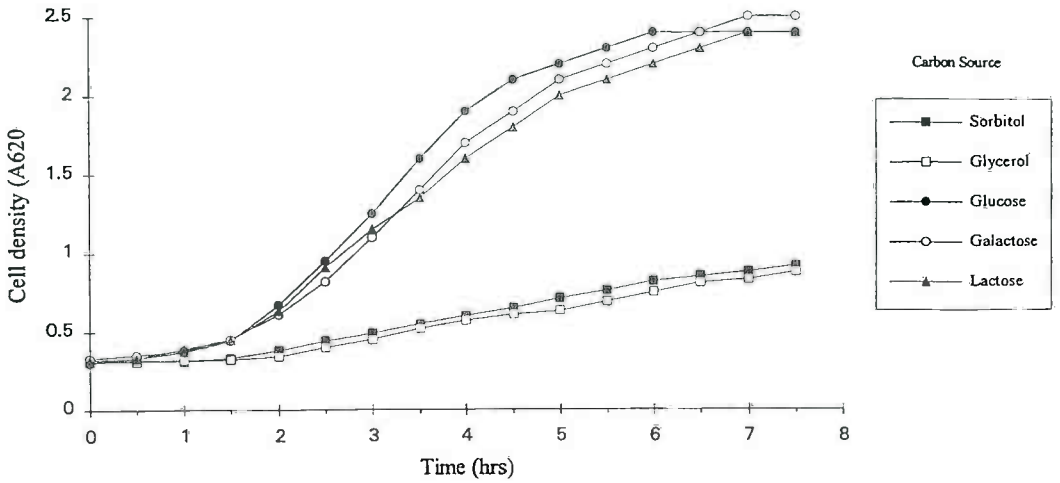

Figure 18 Effect of carbon source on the growth of *K. marxianus*.

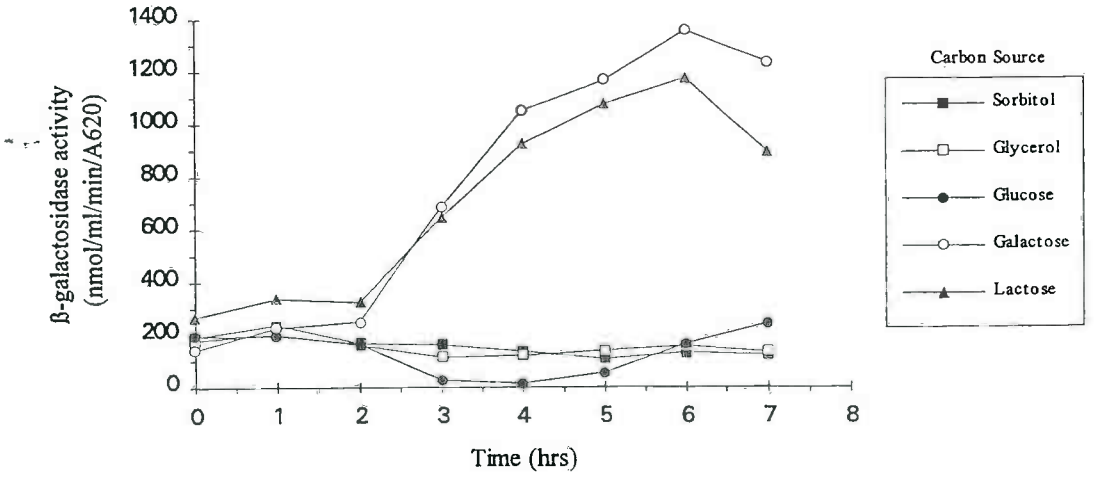

Figure 19 Effect of carbon source on β-galactosidase activity in *K. marxianus*.

Carbohydrate	β-galactosidase activity (relative values)	
	Carbohydrate used as :-	
	Sole carbon source	Inducer
Sorbitol	1.00	1.00
Glycerol	1.02	n.d.
Glucose	1.83	n.d.
Lactose	6.73	7.61
Galactose	9.20	8.01
ϕTG	n.d.	1.18
MTG	n.d.	1.2
IPTG	n.d.	1.22

n.d. = not determined

Table 38 Relative effect of inducers on expression of β-galactosidase by *K. marxianus*. Where the carohydrate was used as an inducer media also contained 20mM sorbitol as carbon source.

This study established induction conditions for the expression of β-galactosidase in *K. marxianus* and showed that sorbitol, glycerol, and the gratuitous inducers of β-galactosidase in *E. coli*, could not be used for the induction of β-galactosidase in *K. marxianus;* lactose and galactose however, could be used to induced enzyme activity whereas glucose caused the repression of β-galactosidase.

However, the use of ONPG as a colorimetric substrate in the prospective bioassay was limited. The cleavage product is yellow and has an absorbance peak at 420nm, at which growth medium also absorbs; the determination of enzyme activity therefore required the transfer of cells to Z-buffer prior to enzyme determination. This step would make the prospective bioassay rather labour intensive and an alternative chromogenic substrate (which absorbs outside the absorbance range of growth media) was desirable for the development of a simple colorimetric bioassay.

3.1.2 EVALUATION OF ALTERNATIVE CHROMOGENIC SUBSTRATES

Two chromogenic substrates were assessed for use in the development of a colorimetric bioassay. The first, 5-bromo-4-chloro-3-indolyl-β-D-galactopyranoside (Xgal) is a substrate for β-galactosidase, used for the histochemical determination of emzyme activity (section 1.4.2); the cleavage of Xgal produces an indigo product which is an insoluble blue precipitate (Figure 11, page 59). The second, 3-(4,5-dimethylthiazol-2-yl)-2,5-diphenyl tetrazolium bromide, (MTT), is a tetrazolium salt.

3.1.2.2 MTT

The ability of *K. marxianus* to cleave MTT was determined using whole cells, as detailed in section 2.2.2.3. Whole cells were able to cleave MTT to its formazan product within 4 hours. The absorbance spectrum of the formazan product of cleaved MTT is shown in Figure 23 and shows a broad peak between 450 and 690nm with an absorbance maximum at 560 nm.

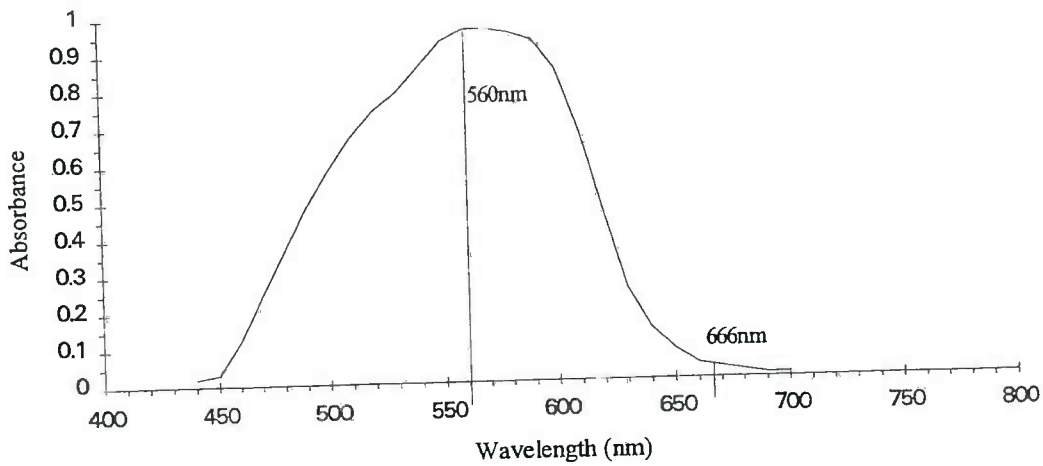

Figure 23 Absorbance spectrum of the formazan product of cleaved MTT.
560 and 666nm are the wavelengths of the filters used for the determination of cell viability in the microtitre plate assay described later (see page 115).

As can be seen from Figures 22 and 23, both Xgal and MTT absorbed at wavelengths outside those at which growth media absorbs (growth media absorbing at wavelengths below 500nm), and both substrates therefore offered potential as colorimetric substrates in the bioassay.

3.1.3 MINIATURISATION OF THE BIOASSAY BY THE USE OF MICROTITRE PLATE TECHNOLOGY.

The use of microtitre plate technology in the development of the bioassay methodology was attractive as it allows a large number of replicate samples to be analysed simultaneously under identical experimental conditions, data can be obtained rapidly compared to spectrophotometric readings, and it is more cost effective due to the smaller sample volumes.

A microtitre plate reader is a microprocessor controlled photometer designed to measure light absorbance (optical density) of samples in a microtitre plate. It can operate in either single or dual wavelength mode, measurement of the absorbance of a sample at two wavelengths being conventionally used to eliminate errors caused by imperfections (e.g. dirt and scratches) on the base of the plate. The selection of a combination of test and reference filters is dependent on the enzyme/substrate system that is being measured. The wavelength of the test filter, (λt), should be at (or within) the absorbance peak of the product; whereas the wavelength of the reference filter, (λr), should be at just outside the absorbance peak. The subtraction of the absorbance at λr from the absorbance at λt being used to reduce systematic errors.

The use of microtitre plate readings for the measurement of cell density and the determination of β-galactosidase activity (cleavage of Xgal) and cell viability (cleavage of MTT) was determined as detailed in section 2.2.3. Test and reference filters used in the microtitre plate reader were selected following analysis of the absorbance spectra of cleaved Xgal (Figure 22) and cleaved MTT (Figure 23).

As can be seen from these two figures, the indigo product of cleaved Xgal showed a broad absorbance peak between 500 and 800nm, where as the formazan product of the cleavage of MTT was found to absorb between 450 and 690nm. The absorbance produced by media and cells was found to be relatively constant above 500nm (data not shown). Using filters at 560 and 666nm, both β-galactosidase activity (cleavage of Xgal) and cell viability (cleavage of MTT) could be detected using the microtitre plate

reader. The absorbance resulting from cleaved Xgal was determined using a test filter at 666nm and a reference filter at 560nm and the abosrbance resulting from cleaved MTT determined using a test filter at 560nm and a reference filter at 666nm. Cell density was determined by a single wavelength measurement of the absorbance at 560nm, made prior to either the Xgal or MTT assays.

The miniaturised microtitre plate approach was used for the determination of cell density, β-galactosidase activitiy and cell viability in all subsequent experiment; details are given in the relevant experimental sections.

3.1.4 DETERMINATION OF β-GALACTOSIDASE ACTIVITY USING XGAL

3.1.4.1 Toxicity of dimethylformimide (DMF) to *K. marxianus*

The recommended solvent used to dissolve Xgal is dimethylformimide (DMF) (Sigma chemical Company); the use of Xgal as a colorimetric substrate in the bioassay would therefore expose *K. marxianus* to this solvent, and the toxicity of DMF to *K. marxianus* was determined, as detailed in section 2.2.4.2.

Representative growth curves for *K. marxianus* in the presence of DMF are shown in Figure 24.

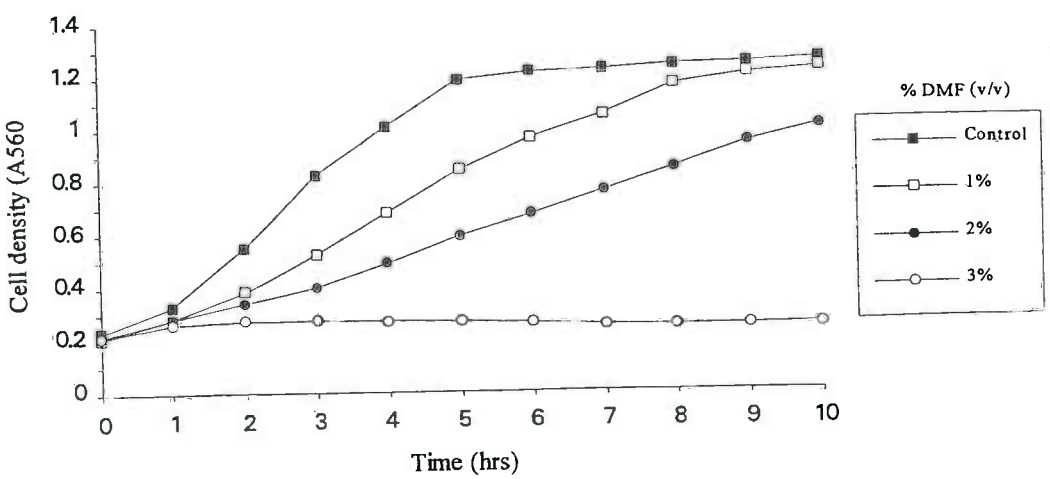

Figure 24 Effect of DMF on the growth of *K. marxianus*.

DMF inhibited the growth of *K. marxianus* at all concentrations tested. As little as 3% (v/v) completely inhibited growth. 1% (v/v) slowed down the rate of growth, but the

final cell density was similar to the control. Consequently, 1% (v/v) DMF was the maximum volume that could be added to the bioassay system without causing a substantial inhibition of growth.

3.1.4.2 Use of Xgal as a chromogenic substrate for the determination of β-galactosidase activity

In any toxicity study it is desirable to keep the responding cell system as intact as possible, (leaving aside any effects due to the toxin being assessed) and the *in vivo* use of Xgal for the histochemical determination of β-galactosidase is well documented (see section 1.4.4). The use of Xgal as the chromogenic substrate for β-galactosidase was therefore attractive as it offered the possibility of the detection of enzyme activity without the use of the permeabilisation step necessary in the ONPG assay. Consequently, initial studies examined the cleavage of Xgal by whole lactose-grown cells as detailed in section 2.2.4.3.

Using whole cells, the appearance of the blue indigo product produced by the enzymatic cleavage of Xgal took over 24 hours. However, the results obtained using the ONPG assay (Figure 19, page 108) indicated that a high level of β-galactosidase activity occur in the cells after 7 hours growth - this being undetectable using whole cells and Xgal. The limiting step appeared to be the uptake of Xgal, as following the reintroduction of the permeabilisation step, used in the ONPG assay, the blue cleavage product of Xgal was clearly visible after 30 minutes incubation.

The indigo product produced by the cleavage of Xgal is a blue precipitate and is insoluble in aqueous solutions, making quantitative determination of β-galactosidase activity difficult. However using the microtitre plate reader in dual wavelength mode, errors in absorbance measurements due to light scattering (caused by both the indigo precipitate and the yeast cells) were eliminated by the use of the reference wavelength measurement (see section 3.1.3) and a semi-quantitative measurement of β-galactosidase activity could be made. In subsequent experiments β-galactosidase activity is expressed as the cleavage of Xgal (A_{666}-A_{560}) as a function of time (minutes) and cell density (A_{560}).

3.1.4.3 Effect of carbon source on β-galactosidase activity: Xgal as the chromogenic substrate

The effect of lactose, galactose and glucose on growth and β-galactosidase activity of *K. marxianus* was determined using the miniaturised microtitre plate approach and Xgal as the chromogenic substrate for β-galactosidase as detailed in section 2.2.4.4, and is shown in Figures 25 and 26, respectively.

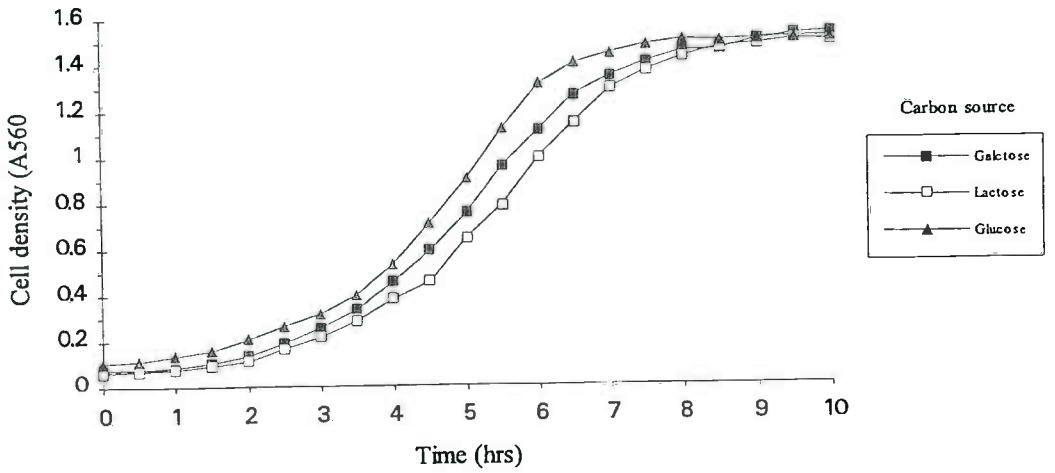

Figure 25 Effect of carbon source on the growth of *K. marxianus*.

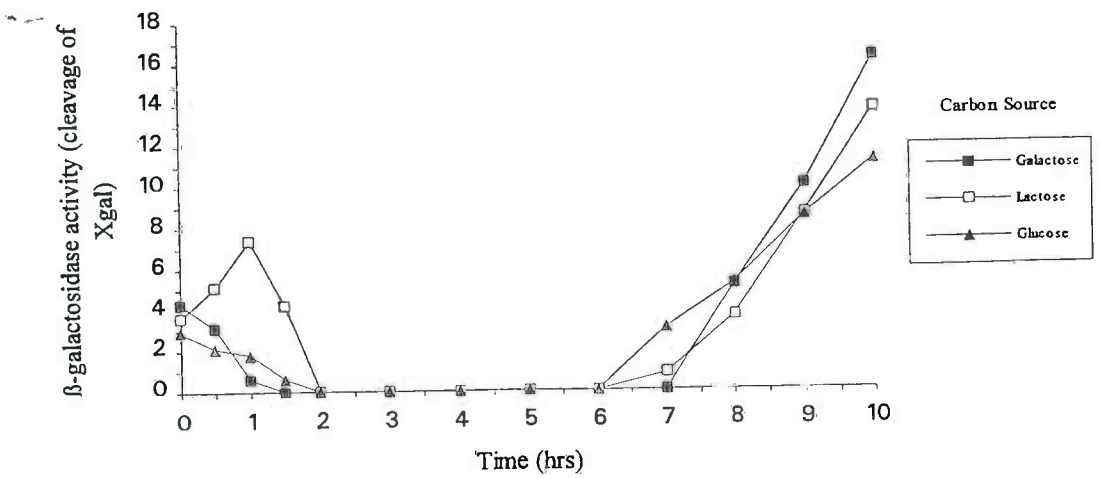

Figure 26 Effect of carbon source on β-galactosidase activity: Xgal as the chromogenic substrate. β-galactosidase activity is expressed as the cleavage of Xgal (A_{666}-A_{560}) as a function of time (minutes) and cell density (A_{560}) x100.

Growth rates of *K. marxianus* on lactose, galactose and glucose determined using the microtitre plate approach (Figure 25) were not significantly different to those obtained using the 50ml shake-flask cultures (in the ONPG assay) (Figure 18, page 108).

Using the microtitre plate approach and Xgal for the determination of β-galactosidase activity, glucose was found to repress β-galactosidase activity throughout the lag phase, until the cells entered the log phase of growth when levels became almost undetectable. Enzyme activity remained repressed throughout the log phase, but, as the cells entered stationary phase enzyme activity became derepressed (Figure 26). In this respect, the determination of β-galactosidase activity in glucose-grown cultures was fairly similar when using Xgal (Figure 26) and ONPG (Figure 19, page 108) as the chromogenic substrate for β-galactosidase. However, the levels of activity determined using the two chromogenic substrates did show some variations. When using Xgal as the chromogenic substrate for β-galactosidase the levels of activity appeared to be repressed for a longer period of time (5 hours when using Xgal compared to only 1 hour when using ONPG), and to a lower level (repressed levels of activity being undetectable using Xgal compared to levels of approximately 20nmol/ml/min/A_{620} using ONPG). This seems to indicate that there is a greater sensitivity of detection when using ONPG compared to Xgal for the detection of β-galactosidase.

Furthermore, using Xgal, the derepression levels of activity (seen in glucose-grown cultures as the cells enter stationary phase) were comparable to levels of activity in lactose and galactose-grown cultures at the same stage in the growth cycle (Figure 26), but were approximately 3 times lower than those in lactose- or galactose-grown cultures when using ONPG (Figure 19).

Levels of β-galactosidase activity seen in galactose-grown cultures when using Xgal as the chromogenic substrate (Figure 26) were broadly similar to those of glucose-grown, with enzyme activity being repressed during the lag and log phases and derepressed as the cells entered stationary phase. However, activity in galactose-grown cultures was derepressed more rapidly and reached higher levels than in glucose-grown cultures

(Figure 26). This contasts sharply with levels of activity in galactose-grown cultures determined using ONPG (Figure 19); the repression of enzyme activity seen using Xgal is not seen when using ONPG, and when levels of activity are undetectable (between 2 and 7 hours of the growth cycle) using Xgal, induced levels of enzyme activity are detected using ONPG.

Enzyme activity for lactose-grown cells determined using Xgal was very similar to that seen in galactose-grown cells, with the exception of a peak in enzyme activity after one hour (Figure 26). This peak does not occur for any other substrate or when determination is made using ONPG (Figure 19). However, the peak in enzyme activity rapidly disappeared, and activity was repressed (as seen with glucose and galactose) until stationary phase was entered. The cause of this peak in activity is unknown, but Xgal was shown not to act as an inducer of β-galactosidase in *K. marxianus* (data not shown).

Final levels of enzyme activity for the three carbon sources, determined using Xgal, showed a similar trend to those determined using ONPG, with maximal levels being induced by galactose, followed by lactose and lower levels being induced by glucose.

The disparity in data between determinations using Xgal and ONPG was unexpected and remains unresolved. It was presumed that the two chromogenic substrates would provide broadly similar results and due to this disparity in the results, lactose and galactose were considered to be unsuitable as inducers of β-galactosidase in a bioassay using Xgal as the chromogenic substrate.

Though glucose is not an inducer of β-galactosidase, de *novo* synthesis of β-galactosidase does occur in glucose cultures. During the lag phase of growth, glucose represses enzyme activity that is initially present in the cells and then as the medium becomes exhausted of glucose and the culture reaches stationary phase, the absence of glucose in the medium triggers the derepression of enzyme activity which involves the *de novo* synthesis of this enzyme.

Therefore, using Xgal and glucose, a simple colorimetric bioassay system was available. Any toxin that interfered with the derepression of *de novo* synthesis of β-

galactosidase activity in glucose cultures could be detected by the inability of the culture to cleave Xgal, as compared to a control not containing toxin.

3.1.4.4 Optimisation of the Xgal assay

3.1.4.4.1 Effect of concentration of Xgal on rate of cleavage

As an enzyme substrate, for the accurate determination of β-glactosidase activity, Xgal must be present in excess. The effect of substrate (Xgal) concentration on β-galactosidase activity was assessed as detailed in section 2.2.4.5.1 and the results are shown in Figure 27.

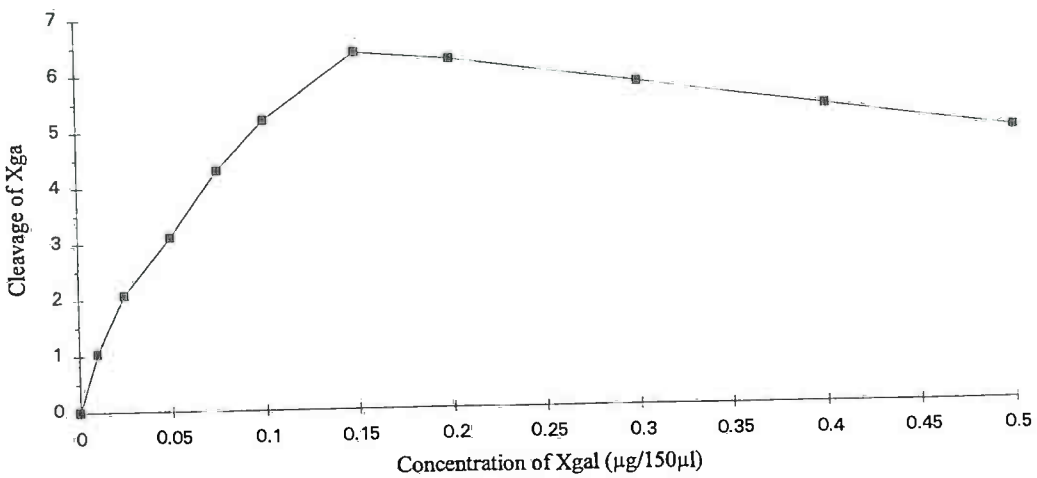

Figure 27 Effect of concentration of Xgal on the rate of cleavage of Xgal by β-galactosidase. Cleavage of Xgal = A_{666}-A_{560}/time/cell density (A_{560}) x100.

There was an almost linear increase in the rate of cleavage with increasing substrate concentration up to 0.15µg/150µl; above this concentration, further increases in substrate concentration caused a slight decrease in rate. Xgal was therefore routinely used at a final assay concentration of 0.15µg/150µl in all subsequent experiments.

DMF is itself toxic to the yeast (section 3.1.4.1) and although enzyme activity was to be determined after growth was complete, it was desirable to keep the amount of DMF present to a minimum and the use of solutions of Xgal in aqueous DMF was assessed

using ratios of water:DMF of 4:1, 3:2, 2:3, and 1:4. Xgal was found to be insoluble in solutions of 4:1 and 3:2 (water:DMF). The rate of cleavage of Xgal in solutions of water:DMF (2:3) was found to be not significantly different to that using 100% DMF (data not shown), and Xgal was therefore routinely added to the bioassay at a concentration of 0.15µg/150µl using a stock solution of 20mg/ml in aqueous DMF (2:3).

3.1.4.4.2 Effect of glucose concentration on β-galactosidase activity in *K. marxianus*

The effect of variations in the glucose concentration of the medium on the repression and derepression β-galactosidase activity in *K. marxianus* was determined as detailed in section 2.2.4.5.2 and is shown in Figure 28.

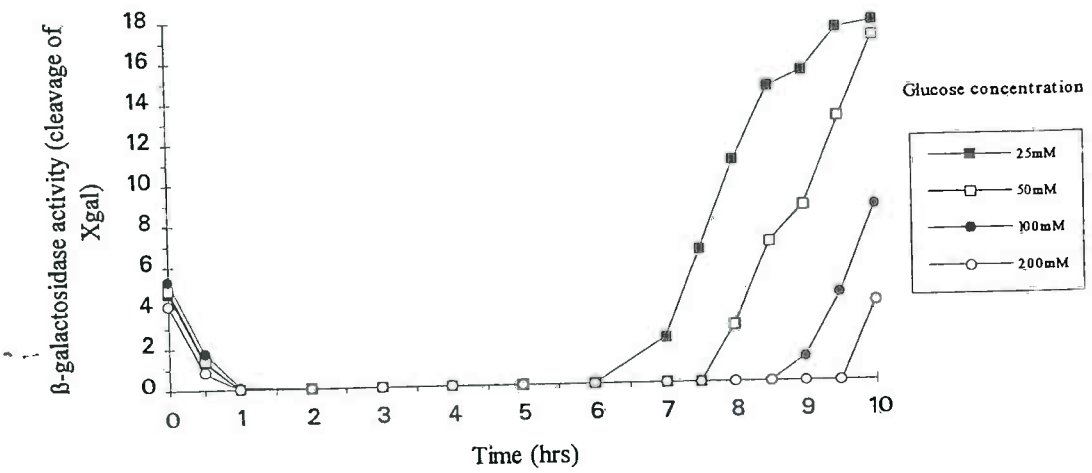

Figure 28 Effect of glucose concentration on β-galactosidase activity in *K. marxianus*. β-galactosidase activity is expressed as the cleavage of Xgal (A_{666}-A_{560}) as a function of time (minutes) and cell density (A_{560}) x100.

The variations in glucose concentration had no effect on the initial repression of enzyme activity, with activity at all concentrations tested being repressed after one hour of growth; however, increasing glucose concentrations did delay the derepression of enzyme activity to a later stage in the growth cycle (Figure 28). Glucose inhibits

β-galactosidase activity through catabolite repression, and the delay in the derepression seen in Figure 28 is a reflection on the increased length of time needed to deplete glucose concentrations in the medium to the critical level at which β-galactosidase activity is derepressed. Derepressed levels of enzyme activity (seen after 10 hours of growth) were similar for glucose concentrations of 25 and 50mM, but were significantly lower at concentrations of 100 and 200mM. It was desirable to obtain results using the bioassay as rapidly as possible and medium containing 50mM glucose was therefore routinely used in all subsequent experiments.

3.1.4.4.3 Effect of variations in cell density on β-galactosidase activity in *K. marxianus*

The effect of variations in cell density on the derepression of β-galactosidase activity in *K. marxianus* was determined as detailed in section 2.2.4.5.3. Cultures of varying cell densities were prepared by the dilution of the inoculation culture of 1:50, 1:20, 1:10 and 1:5 into fresh medium, thereby giving starting cell densities of 4 x 10^7, 1 x 10^8, 2 x 10^8 and 4 x 10^8 cells/ml, respectively. The effect of cell densitiy on β-galactosidase activity in *K. marxianus* is shown in Figure 29.

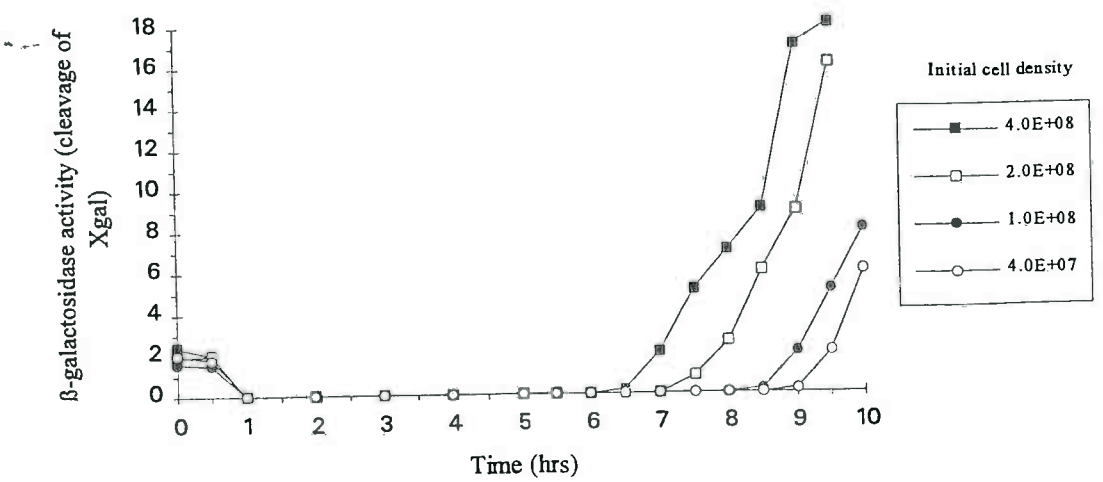

Figure 29 Effect of variations in cell density on β-galactosidase activity in *K. marxianus*. β-galactosidase activity is expressed as the cleavage of Xgal (A_{666}-A_{560}) as a function of time (minutes) and cell density (A_{560}) x100.

Repression of enzyme activity was not affected by the varitaions in the cell densitiy, with inital activity being repressed after 1 hour for all cell densities tested (Figure 29). However, variations in cell density did have an effect on the derepression of enzyme activity observed as the culture reached stationary phase (Figure 29), activity in cultures with higher initial cell densities becoming derepressed more rapidly than those with lower cell densities. This is due to the rate of utilisation of glucose by the cells, which is affected by number of cells present. At lower cell densities glucose is being utilised by fewer cells and is therefore depleted from the medium at a slower rate than will occur when a greater number of cells are present. In cultures with lower cell densities the glucose concentration of the media will therefore reach the critical level at which β-galactosidase activity is derepressed at a later stage in the growth cycle. The results using the bioassay were required as soon as possible and a starting cell density of approximately 2 x 10^8 cells/ml (produced by a 1:10 dilution of the inoculation culture into fresh media) was therefore used in all subsequent experiments.

3.1.5 TOXICITY OF METHANOL AND ETHANOL TO *K. MARXIANUS*

Mycotoxins are generally soluble in polar solvents, but insoluble in non-polar solvents. A polar solvent, which should be miscible with the aqueous growth medium, was therefore necessary to dissolve the mycotoxin and introduce it into the bioassay system. A variety of solvents may be used for this purpose including methanol, ethanol, acetone, dimethylsulphoxide and acetonitrile. A previous study by Dell, (1993), indicated that methanol and ethanol were the least toxic of these to *K. marxianus* and the effects of methanol and ethanol on growth and β-galactosidase activity of *K. marxianus* was therefore investigated here, as detailed in section 2.2.5. Growth curves for *K. marxianus* in the presence of methanol and ethanol are shown in Figures 30 and 31 respectively, from which dose-response curves for the inhibition of growth (at 10 hours) were constructed (section 2.3.5.1); β-galactosidase activity was determined after 10 hours growth and this data used to construct dose-response curves for the inhibition of β-galactosidase activity (section 2.3.5.1) ; all dose-response curves are shown in Figure 32.

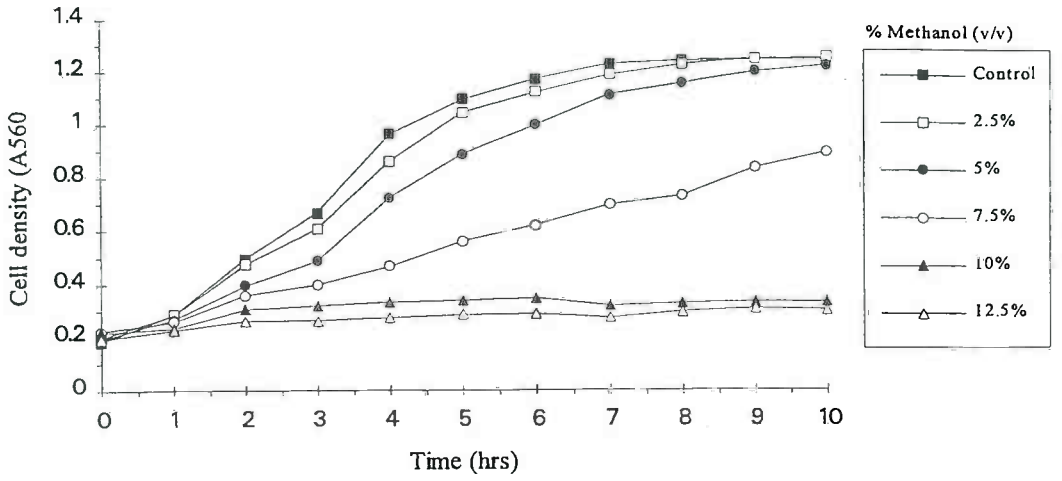

Figure 30 Effect of methanol on the growth of *K. marxianus.*

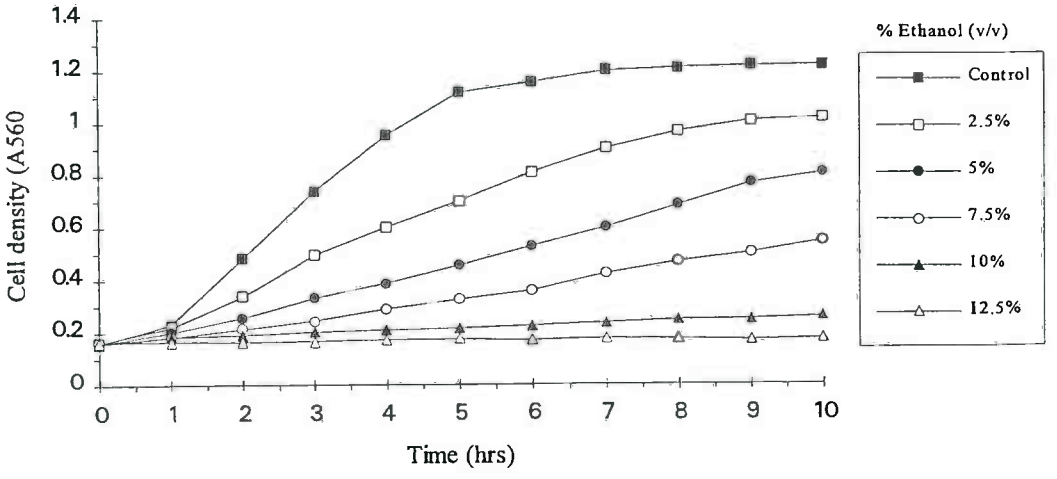

Figure 31 Effect of ethanol on the growth of *K. marxianus.*

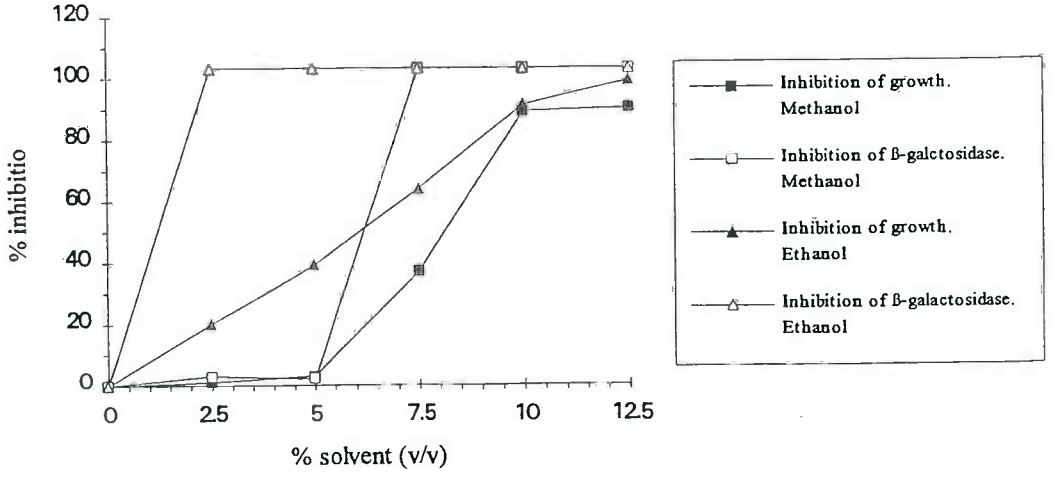

Figure 32 Dose-response curves showning inhibition of growth and β-galactosidase activity of *K. marxianus* by ethanol and methanol.

Ethanol was found to be very toxic to *K. marxianus*, growth being inhibited to some extent at all concentrations tested, and being completely inhibited at 10% (v/v) (Figure 31); β-galactosidase activity was inhibited completely at all ethanol concentrations tested (Figure 32). Methanol was found to be less toxic than ethanol; concentrations of 2.5% and 5% (v/v) caused a slight inhibition of growth, (Figure 30), but final cell densities, after 10 hours of growth (data used to construct dose-response curves) were similar to that of the control. β-galactosidase activity was completely inhibited by methanol concentrations of ≥7.5% (v/v), no inhibition was seen at concentrations ≤5% (v/v) (Figure 32).

Since 5% (v/v) was the maximum volume of methanol that could be added to the medium without causing a significant inhibition of growth and β-galactosidase activity, mycotoxins were introduced into the bioassay system as a methanol stock solution such that the final methanol concentration was never greater than 5% (v/v).

3.1.6 ENHANCEMENT OF THE SENSITIVITY OF THE BIOASSAY BY THE USE OF MEMBRANE-MODULATING AGENTS (MMAs)

The degree of toxicity of mycotoxins to yeasts is dependent on the ability of the toxin to pass through the yeast cell membrane (Schappert & Khachatourians, 1984b). The ability of three MMAs, cetyl trimethyl ammonium bromide (CTAB), polymyxin B sulphate (PMBS) and polymyxin B nonapeptide (PBN), to enhance the toxicity of a representative trichothecene, verrucarin A, to *K. marxianus* was therefore determined. This toxin was selected as it had been reported, by Dell (1993), to be the most toxic of the trichothecene mycotoxins towards *K. marxianus*.

3.1.6.1 Effect of MMAs on growth and β-galactosidase activity in *K. marxianus*

The effects of the three MMAs on growth and β-galactosidase activity in *K. marxianus* were assessed as detailed in section 2.2.6.1. This data was used to determine the highest concentration of each MMA that could be added to the assay medium, without

causing a significant inhibition of growth and β-galactosidase activity, in subsequent experiments.

Representative growth curves for *K. marxianus* in the presence of various concentrations of CTAB, PMBS and PBN are shown in Figures 33, 34 and 35, respectively. Dose response curves were constructed for each MMA, for the inhibition of growth (at 8 hours) and β-galactosidase activity (determined after 8 hours growth) as detailed in section 2.3.5.1, and are shown in Figures 36 and 37.

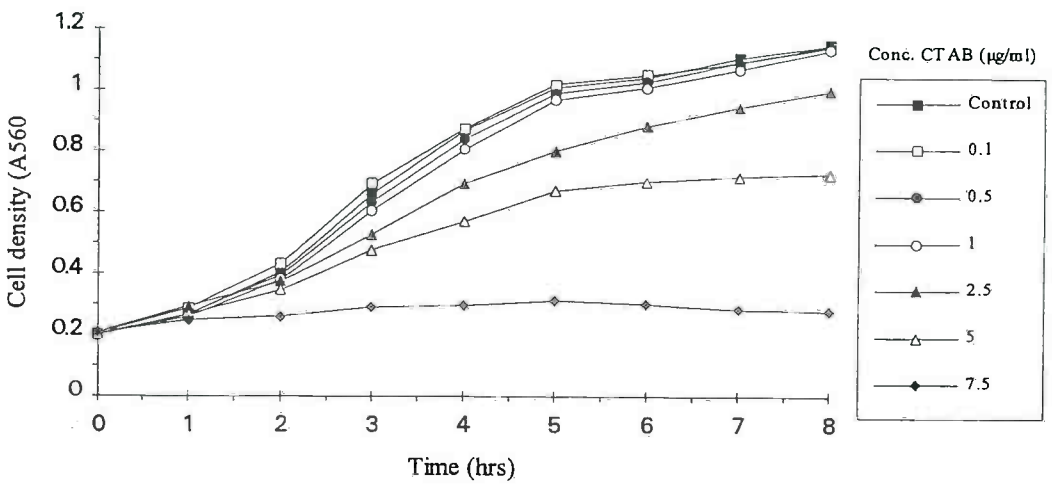

Figure 33 Effect of CTAB on the growth of *K. marxinaus*.

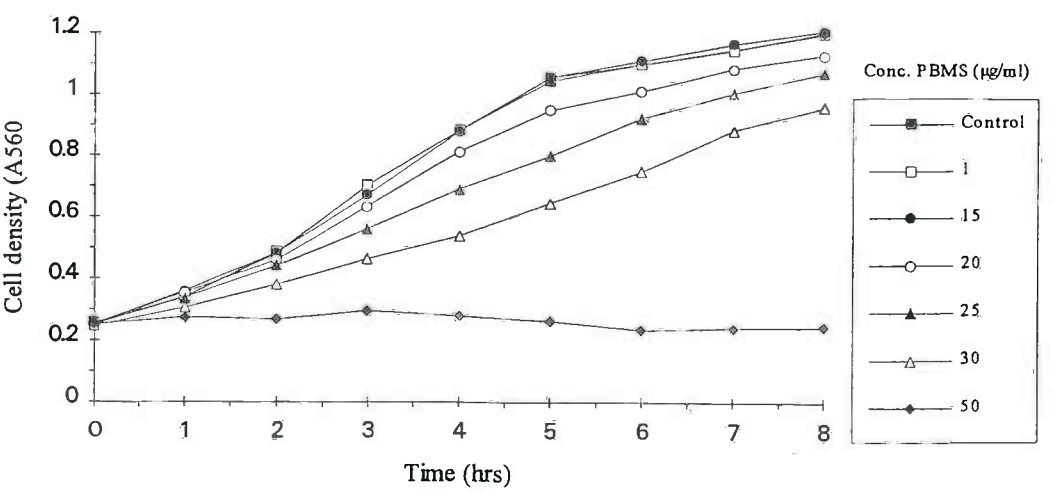

Figure 34 Effect of PMBS on the growth of *K. marxinaus*.

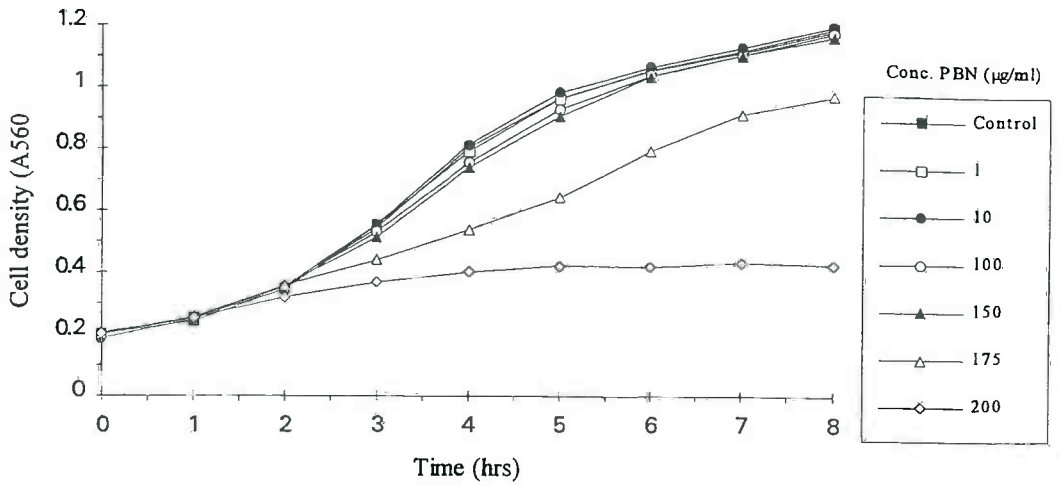

Figure 35 Effect of PBN on the growth of *K. marxinaus*.

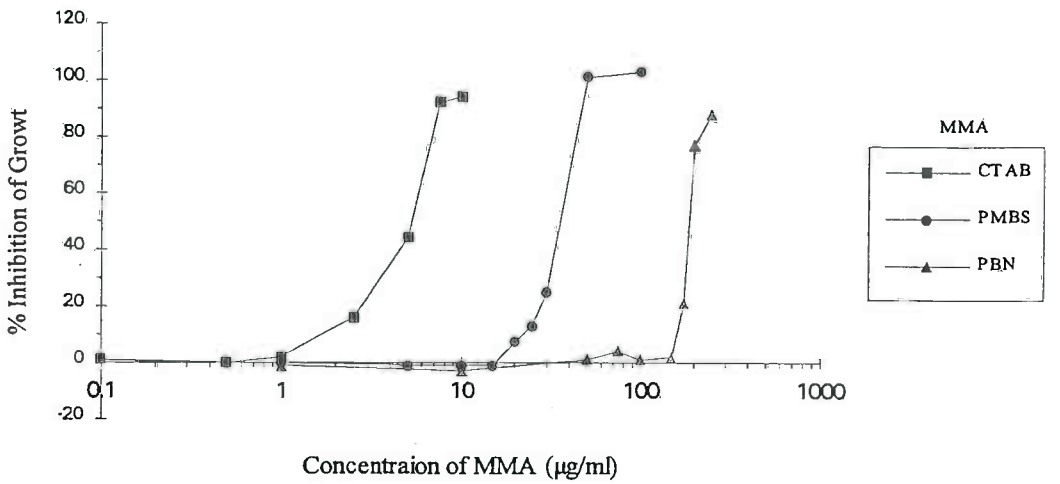

Figure 36 Inhibition of growth by MMAs.

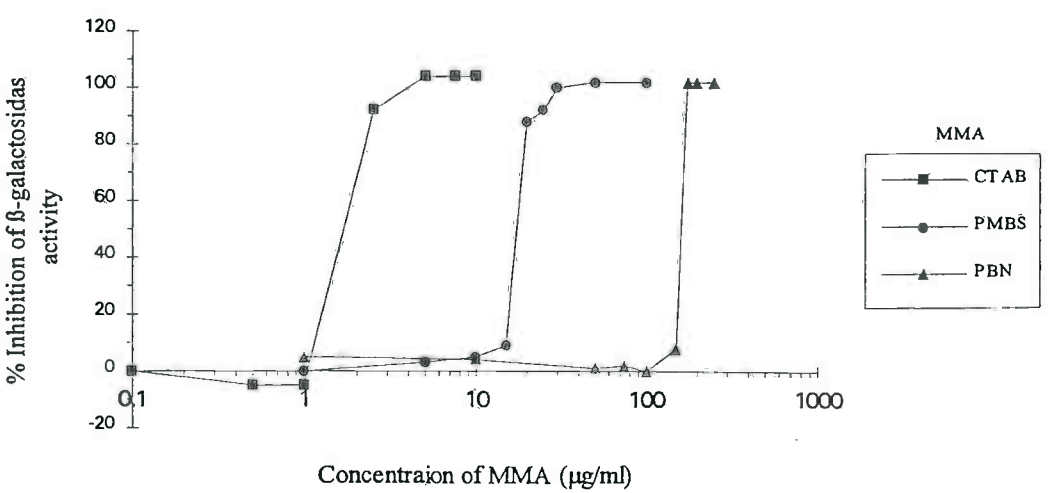

Figure 37 Inhibition of β-galactosidase activity by MMAs.

CTAB was found to be the most toxic of the three MMAs, only concentrations of ≤1μg/ml had no significant inhibitory effect on growth (Figures 33 and 36) or β-galactosidase activity (Figure 37). Higher concentrations were inhibitory, with a complete cessation of growth occurring at ≥7.5μg/ml and β-galactosidase activity being completely inhibited at ≥5μg/ml.

PMBS had no inhibitory effect on growth (Figures 34 and 36) or β-galactosidase activity (Figure 37) at concentrations ≤15μg/ml; however higher concentrations had an inhibitory effect, with complete inhibition of both growth and β-galactosidase activity occurring at concentrations ≥50μg/ml.

PBN was the least toxic of the MMAs assessed; no significant inhibition of growth (Figures 35 and 36) or β-galactosidase activity (Figure 37) was detected at concentrations ≤150μg/ml; higher concentrations did have an inhibitory effect, with a complete inhibition of growth and β-galactosidase activity occuring at concentrations of ≥200μg/ml and ≥175μg/ml, respectively.

The maximum concentration of each MMA that could be added to the assay media without significantly inhibiting growth or β-galactosidase activity of *K. marxianus* was therefore1μg/ml for CTAB, 15μg/ml for PMBS and 150μg/ml for PBN.

The effect of MMAs on the growth of *K. marxinaus* has previously been examined using a disk diffusion assay (Schappert & Khachatourians, 1984b) and a conductimetric bioassay (Connolly & Corry, 1990). In the conductimetric assay, toxicity was detected as changes in the conductance of the media using a Malthus AT 192 conductimetric instrument, and was expressed as changes in peak response time (PRT - the time at which the maximum rate of conductance change occured) in comparison to a control.

In this study it was found that the maximum amount of CTAB that could be added to the medium without inhibiting growth or β-galactosidase activity was 1μg/ml. This is comparable to the other studies, in which 0.5μg/ml CTAB was found to be the maximum concentration which could be used in the disk diffusion assay without

having an inhibitory effect on growth (Schappert & Khachatourians, 1984b) whereas the addition of 1μg/ml CTAB to the conductimetric bioassay was slightly inhibitory, causing a 35% increase in PRT (Connolly & Corry, 1990).

In the conductimetric bioassay, the maximum concentrations of PMBS and PBN that could be added to the medium without having a detectable inhibitory effect on growth were 25μg/ml (PMBS) and 100μg/ml (PBN). This contrasts somewhat to the results of this study, which showed maximum tolerated concentrations to be 15μg/ml (PMBS) and 150μg/ml (PBN), however, both studies agree that PBN is less toxic than PMBS, which is in turn less toxic than CTAB.

Polymyxin B is an antibiotic produced by *Bacillus polymyxia,* and is toxic to bacterial, fungal and animal cells (Storm *et al.*, 1977). It is composed of a cyclic polypeptide joined to an acyl moiety by an amide bond (Glasby, 1979). Proteolytic cleavage of the amide bond removes the antimicrobial activity of both portions (Chihara *et al.*, 1973), and the non-toxic product, polymyxin B nonapeptide (PBN), has been shown to increase the sensitivity of both bacteria (Chihara *et al.*, 1973; Vaara & Vaara, 1983) and yeast (Boguslawski, 1985, Connolly & Corry, 1990) towards toxicants. Polymyxin B exerts its effects by binding to membranes, destroying osmotic properties and causing the leakage of metabolites from within the cell (Storm *et al.*, 1977). Phosphotidyl ethanolamine is thought to be the target molecule in the cell membrane, forming two bonds with suitable protonated amino residues in polymyxin B. Stabilisation of the peptide to allow this bonding comes from the fatty acyl moiety, which inserts into the hydrophobic interior of the cell membrane (Storm *et al.*, 1977). PBN lacks the hydrophobic anchor present in PMBS, and interactions between the peptide and membrane are fairly transient in nature, which may explain the relative non-toxicity of PBN, in comparison to PMBS.

3.1.6.2 Effect of MMAs on verrucarin A toxicity to *K. marxianus*

The ability of CTAB (1μg/ml), PMBS (15μg/ml) and PBN (150μg/ml) to enhance verrucarin A toxicity in *K. marxianus* was determined as detailed in section 2.2.6.2. The growth of *K. marxianus* was monitored over 10 hours (results not shown), after

which β-galactosidase activity was determined. Dose-response curves were constructed for the inhibition of growth and β-galactosidase activity (as detailed in section 2.3.5.1), and are shown in Figures 38 and 39, respectively. Using the dose-response curves, the NEL, EC_{50} and MIC concentrations of verrucarin A for the inhibition of growth and β-galactosidase activity were determined (section 2.3.5.2) and are summarised in Table 39.

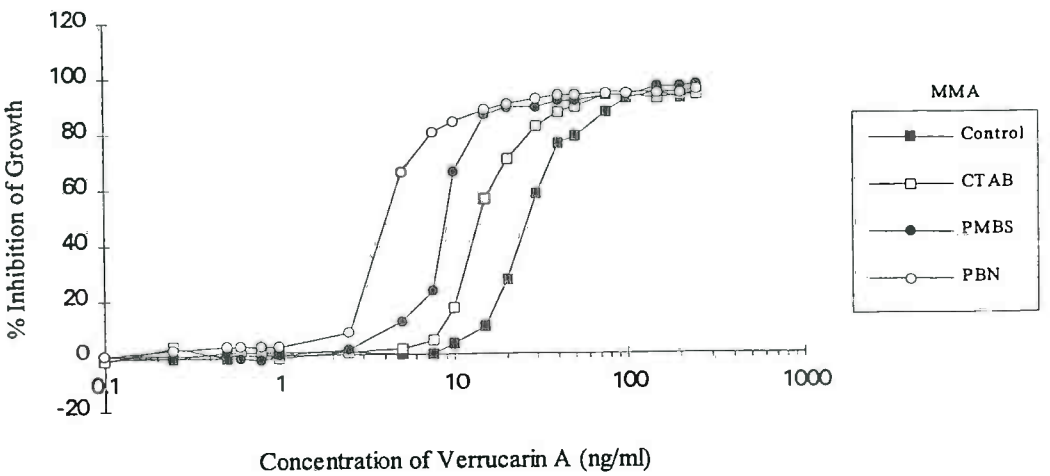

Figure 38 Effect of MMAs on the toxicity of verrucarin A to *K. marxianus* as determined by inhibition of growth.

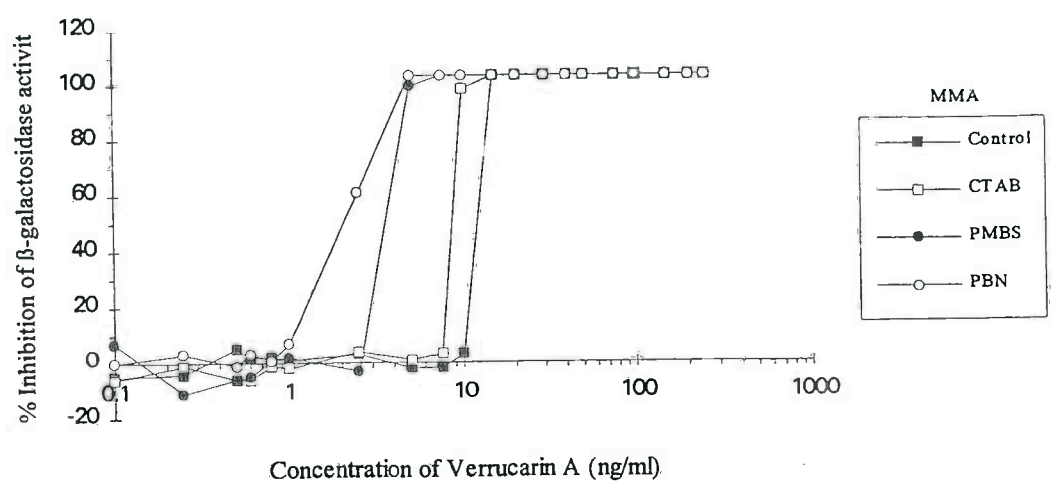

Figure 39 Effect of MMAs on the toxicity of verrucarin A to *K. marxianus* as determined by the inhibition of β-galactosidase activity.

MMA	Inhibition of Growth by verrucarin A			Inhibition of β-galactosidase activity by verrucarin A		
	NEL (ng/ml)	EC_{50} (ng/ml)	MIC (ng/ml)	NEL (ng/ml)	EC_{50} (ng/ml)	MIC (ng/ml)
Control	10	28	100	10	11	15
CTAB (1μg/ml)	5	13	75	7.5	8.5	15
PMBS (15μg/ml)	2.5	9	40	2.5	3.5	7.5
PBN (150μg/ml)	1	4	25	1	2	5

Table 39 Effect of MMAs on verrucarin A toxicity to *K. marxianus*.

As can be seen from Figures 38 and 39 the addition of 1μg/ml CTAB to the media caused only a slight (0- to 2-fold) increase in the sensitivity of *K. marxianus* to verrucarin A in comparison to the control, a more considerable increase in sensitivity (2- to 4-fold) was elicited by 15μg/ml PMBS, but the maximum increase in sensitivity (3- to 10-fold) was elicited by the addition of 150μg/ml PBN. This is further illustrated in the NEL, EC_{50} and MIC concentrations determined for verrucarin A in the presence of each MMA which are given in Table 39.

The use of inhibition of β-galactosidase activity as an endpoint in the bioassay allowed an increase in the sensitivity of detection, when using EC_{50} and MIC values, though not when using NELs as shown in Figures 38 and 39 and in Table 39.

MMAs have been used to enhance the sensitivity of *K. marxianus* to the trichothecenes in a disk diffusion assay (DDA) (Schappert & Khachatourians, 1984b) and a conductimetric bioassay (Connolly & Corry, 1990). These studies both examined the ability of MMAs to increase the sensitivity of *K. marxianus* to a representative trichothecene, T-2 toxin, whereas in this study verrucarin A was used. The effects of MMAs on the sensitivity of *K. marxianus* to verrucarin A , as determined in this study, and to T-2 toxin as determined by Schappert & Khachatourians (1984b) and Connolly & Corry, (1990) are compared in Table 40.

Details of assay procedure		Liquid culture. Inhibition of growth	Liquid culture. Inhibition of β-galactosidase	Disk diffusion assay. Inhibition of growt	Conductimetric assay. Inhibition of growt
Mycotoxin		Verrucarin A	Verrucarin A	T-2 toxin	T-2 toxin
MMA	Paramete used	Effect of MMA on the sensitivity of the assay			
CTAB	NEL	Increased 2-fold, (0.01-0.005μg/ml)	Increased 1.33-fold (0.1-0.075μg/ml)	Not determined	Not determined
	MIC	Increased 1.33-fold (0.1-0.075μg/ml)	No effect (0.015μg/ml)	Increased 10-fold, (2-0.2μg/ml)	Increased 2-fold, (2-1μg/ml)
PMBS	NEL	Increased 4-fold, (0.01-0.0025μg/ml)	Increased 4-fold, (0.01-0.0025μg/ml)	Not determined	Increased 20-fold, (0.1-0.005μg/ml)
	MIC	Increased 2.5-fold, (0.1-0.040μg/ml)	Increased 2-fold, (0.015-0.075μg/ml)	Increased 50-fold, (2-0.04μg/ml)	Increased 200-fold, (2-0.01μg/ml)
PBN	NEL	Increased 10-fold, (0.01-0.001μg/ml)	Increased 10-fold, (0.01-0.001μg/ml)	Not determined	Increased 20-fold, (0.1-0.005μg/ml)
	MIC	Increased 4-fold, (0.1-0.025μg/ml)	Increased 3-fold, (0.015-0.005μg/ml)	Not determined	Increased 200-fold, (2-0.01μg/ml)
Reference		This thesis		Schappert & Khachatourians, 1984b	Corry & Connolly, 1990

Table 40 Ability of MMAs to increase the sensitivity of various yeast bioassays.

As can be seen from Table 40, using the DDA and/or conductimetric assay, PBN was found to elicit the greatest increase in sensitivity followed by PMBS and CTAB; and this is in agreement with this study. However, the increase in sensitivity was much greater in the DDA (up to 50-fold) and the conductimetric assay (up to 200-fold) than in the liquid culture assay (10-fold) described here. It is not possible to compare the overall sensitivity of the liquid culture assay to the disk diffusion and conductimetric assays as different trichothecenes were used (verucarrin A and T-2 toxin) and sensitivity (toxicity) is known to vary with trichothecene structure (see section 3.3.2).

In conclusion, the results of this study clearly showed that MMAs could be used to increase the sensitivity of the bioassay to mycotoxins; PBN was more effective than PMBS, which in turn was more effective than CTAB. The routine use of PBN in the bioassay was ruled out however, due to it's expense. The increase in sensitivity produced by PMBS is only slightly less than that produce by PBN, and PMBS is considerably cheaper than PBN. The cost of an assay kit is of considerable importance and therefore PMBS was routinely used in subsequent bioassay experiments.

T-2 toxin (ng/ml)	Percentage inhibition of growth			Percentage inhibition of β-galactosidase activity			Percentage inhibition of cell viability		
	Exp 1	Exp 2	Exp 3	Exp 1	Exp 2	Exp 3	Exp 1	Exp 2	Exp 3
0.1	2	1	-1	0	4	-12	3	9	-8
1	1	-1	1	0	-7	2	10	0	-10
2.5	3	1	1	8	9	5	82	11	6
5	5	2	4	11	1	20	27	1	23
7.5	7	9	7	91	20	100	40	8	27
10	14	23	16	99	90	103	53	13	36
25	28	51	45	103	103	103	58	58	46
50	61	79	76	103	103	103	71	67	66
75	91	92	90	103	103	103	69	76	81
100	94	93	91	103	103	103	79	76	78
250	97	96	93	103	103	103	81	81	80

Table 41 Inhibition of growth, β-galactosidase activity and cell viability by T-2 toxin, determined in three separate experiments.

Endpoint	Exp 1			Exp 2			Exp 3		
	NEL (μg/ml)	EC_{50} (μg/ml)	MIC (μg/ml)	NEL (μg/ml)	EC_{50} (μg/ml)	MIC (μg/ml)	NEL (μg/ml)	EC_{50} (μg/ml)	MIC (μg/ml)
Growth	1.0	40	100	2.0	24	100	1.0	28	100
β-galactosidase	1.0	6	25	5	8.5	25	0.75	5.8	10
Cell Viability	<0.1	9	>250	1.0	20	>250	1.8	28	>250

Table 42 NEL, EC_{50} and MIC concentrations of T-2 toxin determined from the dose-response curves (Figures 37-39) produced from assays performed on three separate occasions.

For the growth of *K. marxianus*, the within-assay variation was shown to be low with the coefficients of variation (%CV) of replicate wells being <5% in most cases, and <10% in all cases (Tables 1-3, Appendix 1); a coefficient of variation of <10% being taken as an acceptable level of error. When the between-assay variation was assessed the level of variation was found to be much greater, and %CV of >10% were often seen (Table 4, Appendix 1).

Within-assay variation for the determination of β-galactosidase activity was also shown to be low and coefficients of variations were <10% with the exception of samples with very low levels of activity, in which the variation was much greater (Tables 1-3, Appendix 1); however the between assay variation was much greater at all levels of activity (Table 4, Appenidx 1).

In contrast, cell viability, determined by the cleavage of MTT showed both high levels of within-assay (Tables 1-3, Appendix 1) and between-assay (Table 4, Appenidx 1) variation at almost all toxin concentrations tested.

The variation between assays can also be seen in the dose-response curves shown in Figures 40, 41 and 42; again from these it can be seen that the variation was less marked for the inhibition of growth and β-galactosidase activity than for inhibition of cell viability, the latter also being non-linear and showing a great deal of scatter. The calculation of NEL, EC_{50} and MIC concentrations (shown in Table 42) showed that inhibition of β-galactosidase activity gave the most sensitive response, the values obtained from inhibition of growth and cell viability being greater and similar. Although the MTT assay allowed a visualisation of the inhibition of growth it did not allow an increase in sensitivity; and this alongside the the lack of reproducibility, the non-linearity, the increased incubation time required for the MTT assay, (an extra 2-4 hours), and the increased labour intensity, it was decided that the MTT assay did not warrant further development and was not used in subsequent investigations.

The high level of between-assay variation seen for all endpoints may be due to a number of factors which vary between each assay, including cell density of the starting inoculum and possibly more relevant, variations in incubation temperature. Although the plate was incubated in a shaker-incubator in a controlled temperature room, the temperature was found to vary slightly on a day-to-day basis, and this would affect the rate of growth and possibly the inhibitory effect of the mycotoxins on the yeast.

The high level of between-assay variation meant that extra care was needed to be taken when comparing the inhibitory effects and relative toxicities of different mycotoxins, using data obtained in separate experiments. This was a particular problem in the structure-activity study, and in order to obviate this problem, all analysies needed to be performed simultaneously.

3.2.2 DETECTION OF MYCOTOXINS WHICH ARE KNOWN NATURAL CONTAMINANTS OF FOODS AND FEEDS

The toxicity of various mycotoxin standards to the colorimetric yeast bioassay developed in this thesis was determined as detailed in section 2.3.3. Initial studies concentrated on toxins that are known natural contaminants of foods and/or feeds, or reported to be particularly toxic to yeast (Dell, 1993). Of the 14 mycotoxins assessed, only five could be detected using the colorimetric yeast bioassay and the results are summarised in Table 43.

Mycotoxins detected	Mycotoxins not detected, and the maximum concentration tested	
Deoxynivalenol	Aflatoxin B_1	25µg/ml
Diactoxyscirpenol	Aflatoxin M_1	25µg/ml
Roridin A	Cyclopiazonic acid	10µg/ml
T-2 toxin	Fumonisin B_1	10µg/ml
Verrucarin A	Ochratoxin A	10µg/ml
	Patulin	10µg/ml
	Sterigmatocystin	10µg/ml
	Tenuazonic acid	10µg/ml
	Zearalenone	10µg/ml

Table 43 Detection of mycotoxins using the colorimetric yeast bioassay developed in this thesis.

The five mycotoxins that could be detected using the yeast bioassay system (Table 43) are all members of the trichothecene group of mycotoxins; because of this, it was decided to undertake a structure-activity study using a number of the trichothecenes at an expanded range of concentrations. The results of the preliminary study were thus superseded, and dose-response curves and MIC, EC_{50} and NEL concentrations of these toxins are not presented here (but may be seen in section 3.2.3).

None of the non-trichothene mycotoxins assessed using the colorimetric yeast bioassay could be detected at any of the concentrations used (Table 43). Insensitivity of *K. marxianus* to the non-trichothecene mycotoxins has been previously noted using disk diffusion assays: *K. marxianus* was found to be insensitive to AFB_1 (50µg/disk) and zearalenone (20µg/disk) (Schappert & Khachatourians, 1984b), and to AFB_1,

ochratoxin A, citrinin, penicillic acid, cyclopiazonic acid, penitrem A and zearalenone at 200µg/disk and patulin at 10µg/disk (Madhyastha *et al.*, 1994a, b), and these findings are all in accordance with the results of this study (Table 43).

However, the results of this study contrast starkly with the detection of mycotoxins determined using *K. marxianus* in the Bioscreen (Dell, 1993 - data summarised in Table 20, page 54). The Bioscreen system was able to detect 63 mycotoxins, including those not detected using the colorimetric bioassay developed in this thesis and the disk diffusion assays used in other studies (Scappert & Khachatourians, 1984b; Madhyastha *et al.*, 1994a, b). However, using the Bioscreen, classic dose-response curves were not produced, and inhibitory effects were, in many cases, only partial. The exception was in the detection of the trichothecenes, for which complete inhibition was seen at the higher concentrations tested, and results (at these higher concentrations) were comparable to the microtitre plate assay; however, partial inhibitory effects were again seen at the lower trichothecene concentrations tested, this being unrepeatable using the microtitre plate approach of this thesis. There are a number of major differences between the two bioassay system, including media composition, initial cell density, incubation conditions, and the final methanol concentration; this being 5% (v/v) in the microtitre plate assay and 8.5% (v/v) in the Bioscreen assay. Alcohols are well known to increase membrane permeability, and it was thought that the higher methanol concentration used in the Bioscreen assay enhanced the uptake and toxicity of the mycotoxins. This hypothesis is discussed further discussed in Chapter 4; however, the cause of the enhanced sensitivity of detection of many mycotoxins seen using the Bioscreen assay still remains unresolved.

The insensitivity of the colorimetric yeast bioassay to the non-trichothecenes may be due to a number of factors, which may include the lack of toxin entry into the yeast cell; and studies on the uptake and binding of AFB_1 and T-2 toxin by *K. marxianus* and the production of metabolites of these toxins will be described in Chapter 4.

Another reason for insensitvity to some toxins may be the lack or insufficiency of metabolic activation. The aflatoxins, sterigmatocystin and zearalenone are known to require metabolic activation prior to exerting a toxin effect (see sections 1.2.1.3, 1.2.3.6 and 1.2.3.8 respectively), and the sensitivity of many bioassays to these toxins has been previously increased by the use of S9 fraction (rat liver homogenate which contains active cyt P450) (Yates, 1986). It may be that the yeast cyt P450 system does not metabolise these toxins to their active derivatives, resulting in the observed lack of toxicity. This hypothesis will be discussed in Chapter 5; levels of cyt P450 in *K. marxianus* were determined and its ability to bind AFB_1 examined, in comparison to a control of *S. cerevisiae*.

Finally, many toxins show organ specificity in their toxic effects: citrinin and ochratoxin A are primarily nephrotoxins and zearalenone is oestrogenic, and it is therefore perhaps not surprising that a microbial bioassay is unable to detect these toxins.

Interestingly, bacterial bioassays have been shown to be more sensitive in the detection of many of the non-trichothecene mycotoxins than yeast bioassays (see section 1.3.5.1), and many bacterial systems are insensitive to the trichothecenes. The sensitivity, or lack of it, demonstrated by microorganisms to specific groups of mycotoxins may be related to the mode of action of these toxins. In the case of the trichothecenes, they exert their toxic effects by the inhibition of protein synthesis. The mechanism of protein synthesis is similar in prokaryotes and eukaryotes, however the structure of the ribosomes differs. The eukaryotic ribosome consists of a 60S and a 40S subunit, whereas the prokaryotic ribosome is composed of a 50S and a 30S subunit (Stryer, 1981). In both cases peptidyl transferase, (to which the trichothecenes bind, thereby exerting their toxic effects), is an integral part of the larger subunit. It may be that the 50S subunit in bacteria is sufficiently different to the 60S subunit in eukaryotes to confer resistance to the inhibitory effects of the trichothecenes.

3.2.3 STRUCTURE-ACTIVITY RELATIONSHIPS AMONGST THE TRICHOTHECENE MYCOTOXINS

A number of different approaches have been used to study the relative potency of the trichothecenes. These have included dermal toxicity in whole animals (Ueno, 1984), toxicity in an isolated reticulocyte lysate system (Wei & McLaughlin, 1974), inhibition of protein synthesis in cell culture (Thompson & Wannenacher, 1986, Terse *et al.*, 1993), inhibition of growth of *Chlorella* (Ikawa *et al.*, 1985), inhibition of mitochondrial function in *S. cerevisiae* (Schappert *et al.*, 1986), and inhibition of growth of *K. marxianus* using a disk diffusion bioassay (Madhyastra *et al.*, 1994a). These studies have indicated that the most important structural features that affect the biological activity of the trichothecenes are the presence of the 12,13-epoxy ring, the presence of hydroxyl or acetyl groups at appropriate positions on the trichothecene nucleus, the structure and position of side chains, the presence of a second epoxy ring on the trichothecene nucleus and the presence of a macrocycle.

In this study, 13 different trichothecenes were screened, to determine their toxicity in relation to their structural differences, using the colorimetric yeast bioassay developed in this thesis. The trichothecenes were divided into structurally related groups in accordance to Tamm and Tori (1984) (see section 1.2.2) and their effects on the growth and β-galactosidase activity of *K. marxianus* was determined as detailed in section 2.3.4.

The effects of the trichothecenes on the growth of *K. marxinaus* are shown in Figures 2a-2m in Appendix 2. Percentage inhibition of growth at the end of the growth cycle (10 hours), and percentage inhibition β-galactosidase activity was calculated as detailed in section 2.3.1.5 and are summarised in Tables 2a and 2b in Appendix 2. Dose-response curves for the inhibition of growth and β-galactosidase were constructed and are shown in Figures 43, 44, 45, 46, 47 and 48.

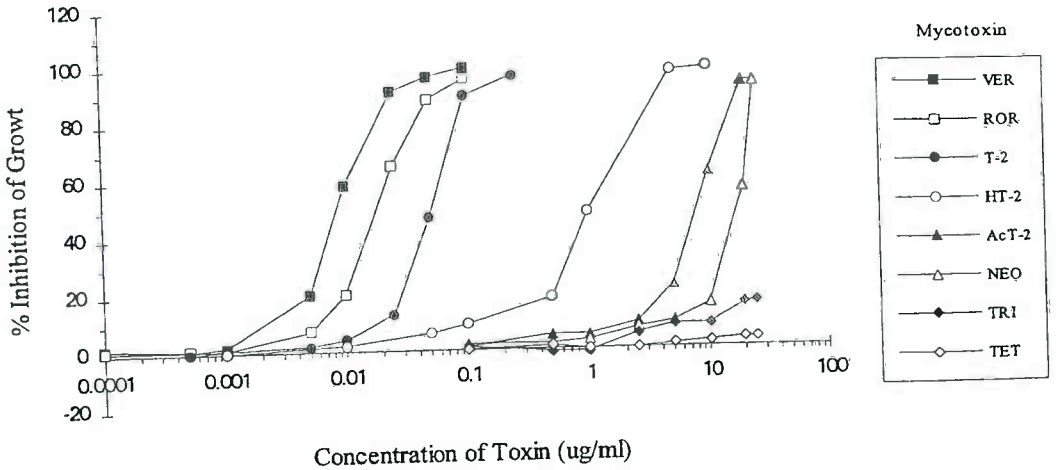

Figure 43 Inhibition of growth by group 1 & 3 trichothecenes.

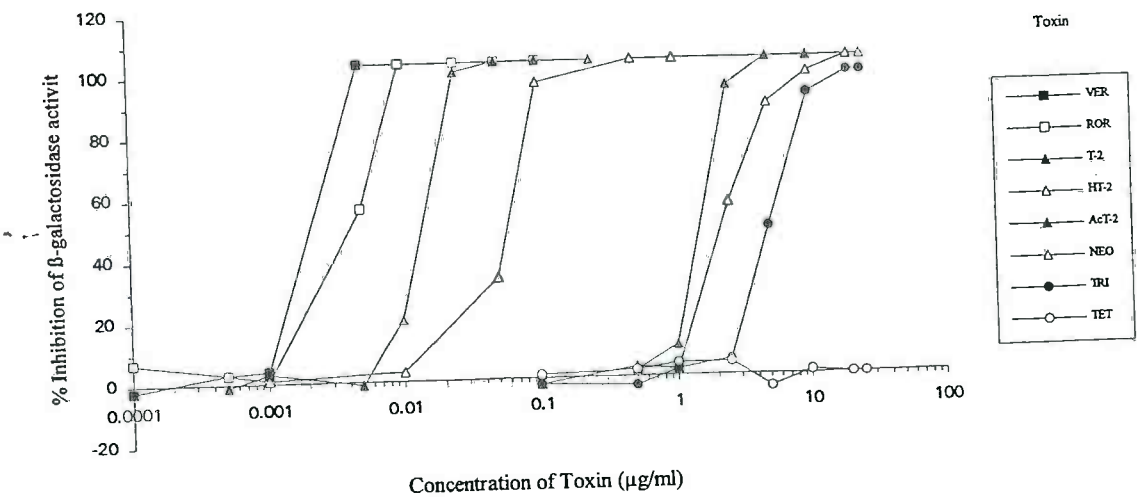

Figure 44 Inhibition of β-galactosidase activity by group 1 & 3 trichothecenes.

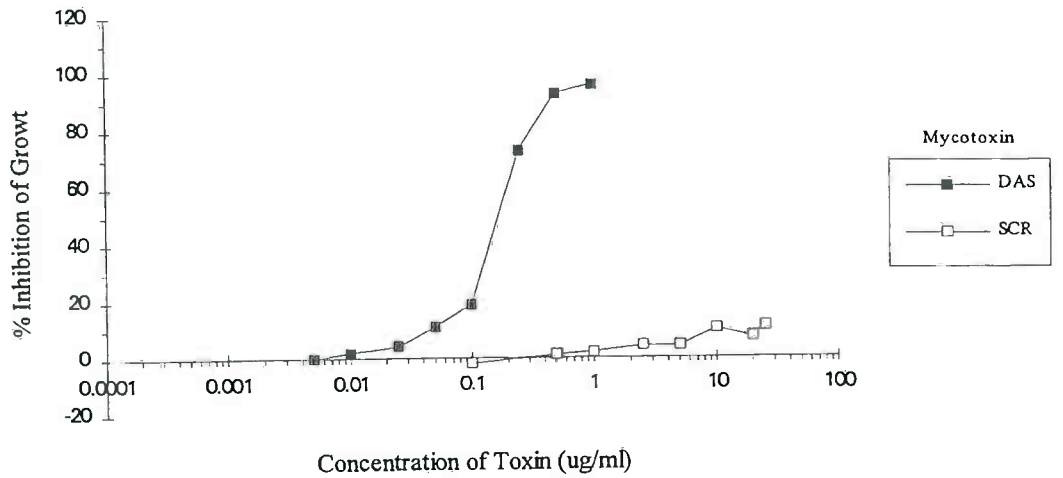

Figure 45 Inhibition of growth by group 2 trichothecenes.

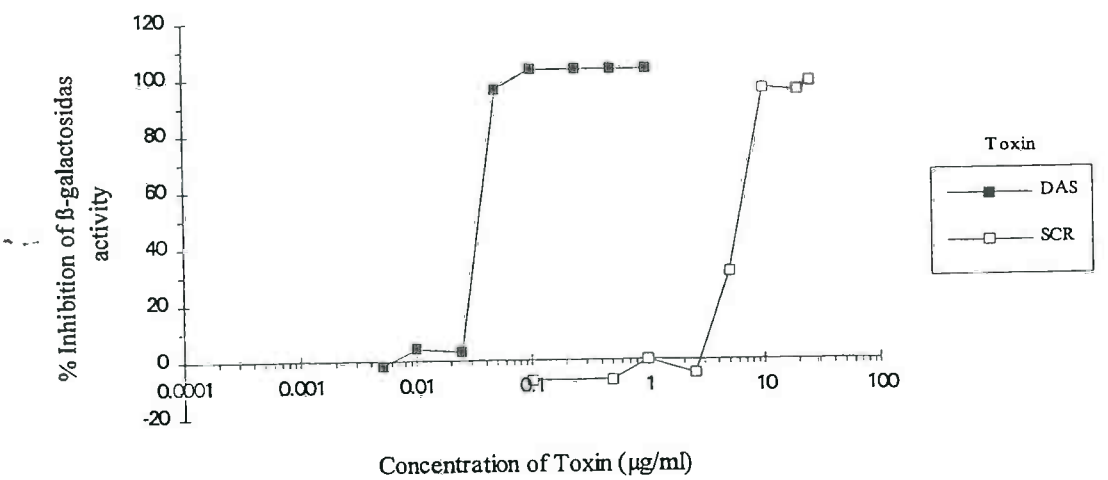

Figure 46 Inhibition of β-galactosidase activity by group 2 trichothecenes.

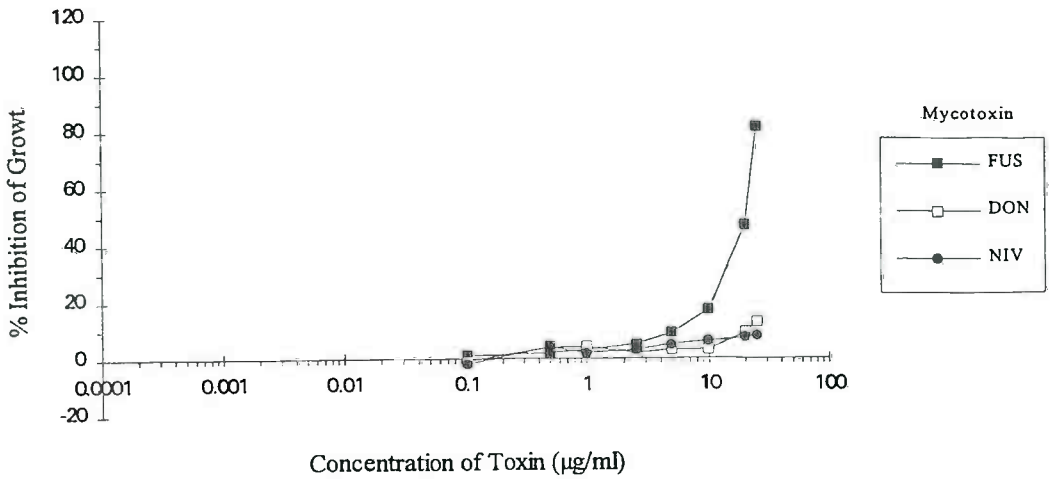

Figure 47 Inhibition of growth by group 4 trichothecenes.

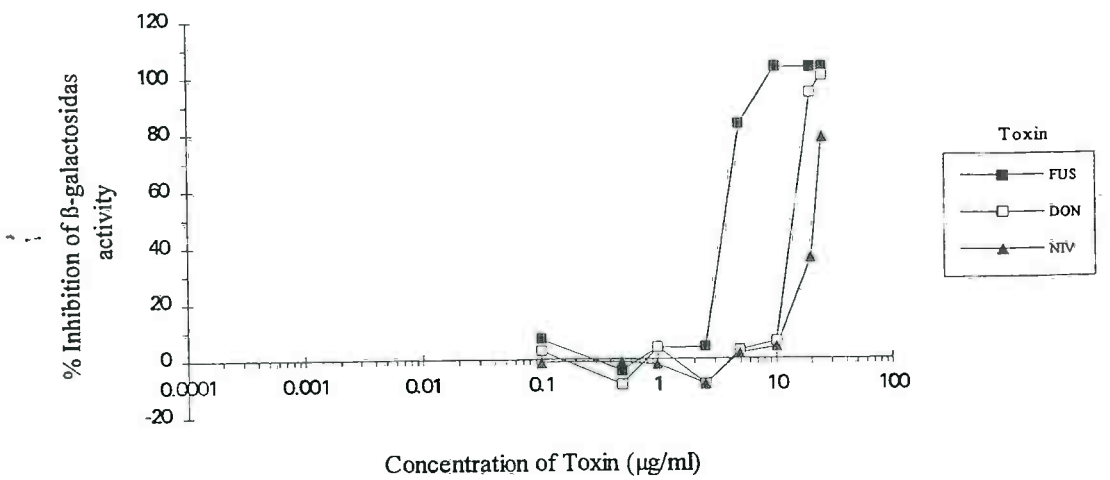

Figure 48 Inhibition of β-galactosidase activity by group 4 trichothecenes.

Using the dose-response curves shown in Figures 43-48, NEL, EC_{50} and MIC concentrations for each toxin were determined as detailed in section 2.3.5.2, and are given in Table 44.

	Inhibition of Growth			Inhibition of β-galactosidase		
Toxin	NEL (μg/ml)	EC_{50} (μg/ml)	MIC (μg/ml)	NEL (μg/ml)	EC_{50} (μg/ml)	MIC (μg/ml)
VER	0.001	0.008	0.1	0.001	0.002	0.005
ROR	0.001	0.018	0.25	0.001	0.004	0.01
T-2	0.001	0.05	0.5	0.005	0.012	0.05
HT-2	0.01	1	5	0.01	0.07	0.5
AcT-2	0.1	8	>25	0.1	1.5	5
NEO	0.5	20	>25	0.5	2	20
TRI	1	>25	>25	0.8	5	>25
TET	>25	>25	>25	>25	>25	>25
DAS	0.005	0.18	1	0.0065	0.03	0.1
SCR	0.1	>25	>25	2.5	6	>25
FUS	0.1	22	>25	0.7	3.5	10
NIV	0.1	>25	>25	4	14	>25
DON	0.1	>25	>25	4	21	25

Table 44 Inhibition of growth and β-galactosidase activity of *K. marxianus* by trichothecene mycotoxins.

Using the data in Table 44, the relative toxicity of the trichothecenes was determined, in relation to verrucarin A - the most toxic of the trichothecenes assayed and is shown in Table 2c in Appendix 2; this analysis gave six separate determinations of the order of toxicity. For the most potent toxins (VER, ROR, T-2, DAS, HT-2 and AcT-2) all six evaluations show agreed on the order of toxicity; however, for the less potent toxins, inhibition was often insufficient to allow the determination of MIC and in some cases the EC_{50} values; which made the exact order of toxicity difficult to determine for some endpoints. The β-galactosidase assay was more sensitive than the growth assay and the relative toxicities of the trichothecenes as determined using inhibition of β-galactosidase is given in Figure 49; the order of toxicity was found to be:-

verrucarin A> roridin A> T-2 toxin> diacetoxyscipenol> HT-2 toxin> acetyl T-2 toxin >neosolaniol> fusarenon-X> T-2 triol> scirpentriol> nivalenol> deoxynialenol> T-2 tetraol.

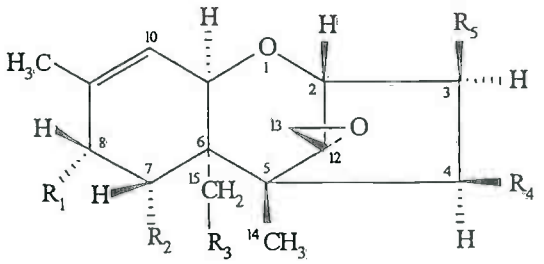

Macrocyclics	R_3 - R_4	*Relative Toxicity
VER	$OC(O)CHOH(CH_3)CH_2CH_2OC(O)CH=CHCH=CHCO$	1
ROR	$OC(O)CHOH(CH_3)CH_2CH_2OC(CHOH)OCH=CHCH=CHCO$	2

Non-macrocyclics	R_1	R_2	R_3	R_4	R_5	
T-2	X	H	$OCOCH_3$	$OCOCH_3$	OH	6
DAS	H	H	$OCOCH_3$	$OCOCH_3$	OH	15
HT-2	X	H	$OCOCH_3$	OH	OH	35
AcT-2	X	H	$OCOCH_3$	$OCOCH_3$	$OCOCH_3$	750
NEO	OH	H	$OCOCH_3$	$OCOCH_3$	OH	1000
FUS	O	OH	OH	$OCOCH_3$	OH	1750
TRI	X	H	OH	OH	OH	2500
SCP	H	H	OH	OH	OH	3000
[illegible]	O	OH	OH	[illegible]	OH	[illegible]
TET	OH	H	OH	OH	OH	>12500

X=$O(CO)CH_2CH(CH_3)_2$

Figure 49 Substituents the trichothecene mycotoxins and their relative toxicity as determined using EC_{50} values for the inhibition of β-galactosidase activity.
***Relative toxicity** = toxin concentration relative to verrucarin A required to elicit an effect as determined using EC_{50} values.

The most potent trichothecenes were the macrocylics (VER and ROR), which have a hydrocarbon chain ring structure between the R_3 and R_4 position. The alcohol group at the C6' position in ROR caused a slight (2-fold) reduction in toxicity compared to the presence of a ketone group in VER.

Of the non-macrocylic trichothecenes, the most potent were those with an acetyl group at the R_3 position (T-2, HT-2, AcT-2, DAS & NEO), with T-2 being the most potent. A pronounced decrease in activity occured with the removal of the acetate group at R_3 (HT-2 to TRI: 71-fold); however, the potency of the trichothecenes was also modified by changes in other substituents around the trichothecene nucleus.

The substitution of the isovaleryl group at R_1 with a hydrogen caused a slight decrease in activity, (T-2 to DAS: 2.5-fold reduction; TRI to SCR: 1.2-fold), whereas substitution with a hydroxyl group caused a more pronounce decrease in activity (T-2 to NEO: 167-fold; TRI to TET: >5-fold). The order of toxicity of the substituents at R_1 therefore being isovaleryl> hydrogen> hydroxyl. This contrasted with substituents at R_4: the substitution of the acetyl group at R_4 with a hydroxyl group resulted in a slight loss of activity (T-2 to HT-2: 6-fold reduction; FUS to NIV: 4-fold reduction); whereas substitution of a hydrogen group resulted in a larger loss of activity (FUS to DON: 6-fold reduction) and the order of toxicity of the substituents at R_4 was therefore acetyl> hydroxyl> hydrogen.

Even more pronounced effects were seen following the substitution the acetyl groups at both R_3 and R_4 with a hydroxyl group (T-2 to TRI: 417-fold reduction; DAS to SCR: 200-fold reduction). The removal of the isovaleryl group at R_1 and the acetyl groups as R_3 and R_4 caused the biggest reduction in toxicity (T-2 to TET: >2083-fold reduction). In contrast, the addition of an acetyl group to the R_5 position caused a decrease in potency (T-2 to AcT-2: 125 fold reduction).

These results are generally in agreement with those from other studies. A study using *K. marxianus* in a disk diffusion assay showed the order of toxicity to be VER> ROR> T-2> HT-2> TRI> TET (Schappert *et al.*, 1986) and T-2> DAS> HT-2> AcT-2> TRI> FUS> DON> NEO> NIV> TET (Madhyastha *et al.*, 1994c). Using the *Chlorella* growth inhibition assay AcT-2 and NEO inhibited growth at 1mg/ml, whereas TET, NIV and DON had no effect (Ikawa *et al.*, 1985). The lymphotoxicity of trichothecenes was shown to decrease with the substitution at the R_4 position; the order of toxicity being acetyl> hydroxyl> hydrogen, (Forsell & Pestka, 1985) which is

3.3 SUMMARY AND CONCLUSIONS

The colorimetric yeast bioassay developed in this thesis can be used for the sensitive detection of the trichothecene mycotoxins; detection limits vary according to the trichothecene being assessed and are given in Table 44 (page 146). Using the yeast bioassay, structure-activity relationships amongst the trichothecenes were determined, the order of toxicity was found to be:

verrucarin A> roridin A> T-2 toxin> diacetoxyscipenol> HT-2 toxin> acetyl T-2 toxin >neosolaniol> fusarenon-X> T-2 triol> scirpentriol> nivalenol> deoxynialenol> T-2 tetraol.

The most important feature affecting biological activity was found to be the substituent at the R_3 position of the trichothecene nucleus; trichothecenes with a hydroxyl group at R_3 were found to be the least potent, and the presence of an acetyl group enhanced toxicity, but the most potent trichothecenes were those with a macrocyclic side chain between R_3 and R_4. The potency of the trichothecenes was also modified by changes in other substituents around the trichothecene nucleus, the order of toxicity at R_1 being isovaleryl> hydrogen> hydroxyl and at R_4 acetyl> hydroxyl> hydrogen, however at the R_5 position, the removal of the acetyl group caused an increase in toxicity.

The yeast bioassay is based on the inhibition of growth of the yeast, *Kluyveromyces marxianus* (strain GK1005); toxicity can be determined by the spectrophotometric determination of cell density using a microtitre plate reader, or by a colorimetric endpoint - the inhibition of β-galactosidase activity determined by the cleavage of Xgal. The use of inhibition of β-galactosidase activity increased the sensitivity of detection compared to inhibition of growth and, perhaps more importantly, enabled the visualisation of toxicity (Figure 50), which allows a qualitative determination of toxicity to be made, in the absence of microtitre plate instrumentation. The bioassay is rapid, simple and offers potential as a field kit; wells containing trichothecene contaminated samples will remain yellow, whereas wells containing non-contaminated samples will turn blue, following the addition of Xgal.

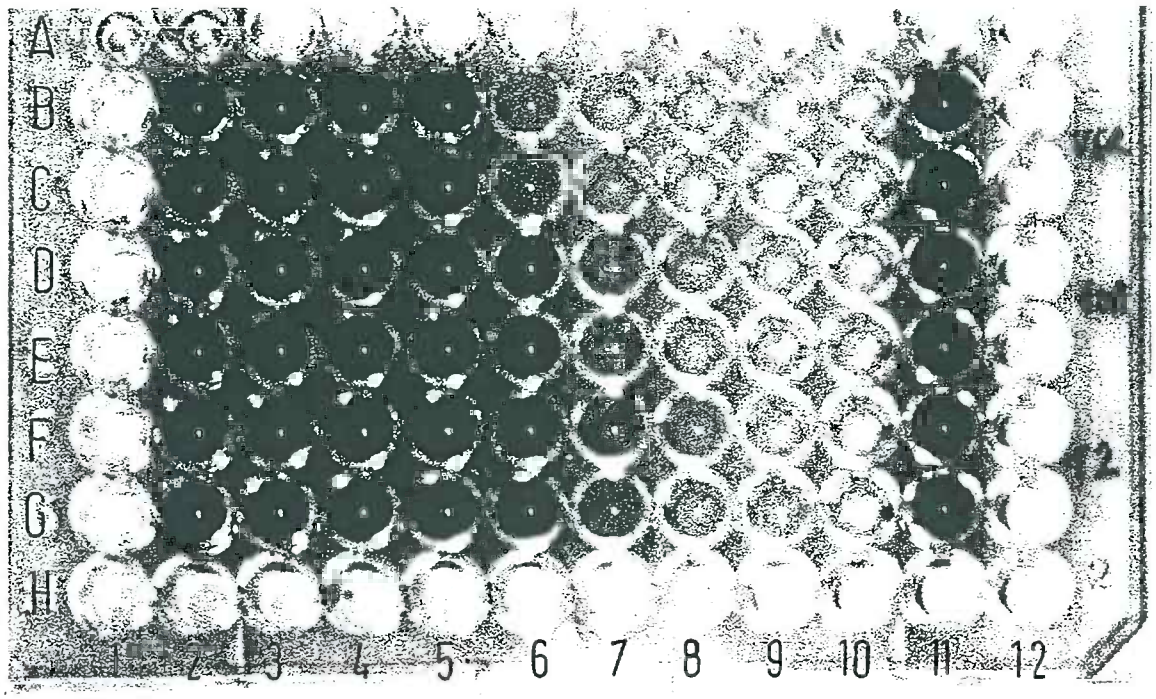

Plate set up - toxin and concentration (ng/ml) in each well.

Rows	Toxin	Columns (toxin concentration ng/ml)											
		1	2	3	4	5	6	7	8	9	10	11	12
B & C	VER	-	Con	0.1	0.5	1.0	5.0	10	25	50	100	Con	-
D & E	ROR	-	Con	0.1	0.5	1.0	5.0	10	25	50	100	Con	-
F & G	T-2	-	Con	0.5	1.0	5.0	10	25	50	100	250	Con	-

Figure 50 Visualisation of toxicity using the yeast bioassay developed in this thesis.
Blue = negative, no inhibition of β-galactosidase activity.
Yelllow = positive, inhibition of β-galactosidase activity.

Although the yeast bioassay, described in this thesis, could be used for the sensitive detection of the trichothecene mycotoxins, it displayed marked insensitivity to other important mycotoxins, such as the aflatoxins (section 3.2.2); and this was in contrast to the results of the Bioscreen assay (Dell, 1993, the findings of which are summarised in Table 20, page 54), which used the same yeast strain, and was able to detect over 60 mycotoxins (including the aflatoxins). The cause of the lack of sensitivity of *K. marxianus* (GK1005) to the aflatoxins was investigated and is described in the following chapters; the possible involvement of methanol in potentiating the sensitivity of the Bioscreen assay is also discussed.

CHAPTER 4

UPTAKE, BINDING AND METABOLISM OF AFLATOXIN B_1 AND T-2 TOXIN BY *K. MARXIANUS* AND *B. MEGATERIUM*

4.1 INTRODUCTION

4.1.1 OBJECTIVES

The yeast selected for the bioassay development work described in this thesis, *K. marxianus* (GK1005), while adequately sensitive to the trichothecene mycotoxins, displayed marked insensitivity to other important mycotoxins such as the aflatoxins (section 3.2.2). One possible reason for the aflatoxin insensitivity could be the lack or insufficiency of an appropriate (cyt P450) activating system, as discussed in Chapter 5; insensitivity may also be due to the lack of toxin entry into the yeast cells. To further clarify this issue, it was decided to examine the uptake of two mycotoxins, T-2 toxin and AFB_1 by *K. marxianus* (GK1005) and to look directly for the production of any metabolites of these toxins. For comparative and control purposes, similar experiments were performed using the bacterium *Bacillus megaterium* (NRRL 1368). This bacterium has been shown to contain an active cyt P450 system (Narhi & Fulco, 1987) and has been reported to be sensitive to AFB_1 and not to T-2 toxin in disk diffusion assays (Tiwari *et al.*, 1985; Clement, 1968a,b; Jayaraman *et al.*, 1968; Lillehoj & Ceigler, 1968).

A key element in the work described above is the use of quantitative analytical techniques. Numerous quantitative methods may be used for the estimation of mycotoxins including thin layer chromatography (TLC), high performance TLC (HPTLC), high performance liquid chromatography (HPLC), immunoassay, mass spectrometry, gas chromatography and fluorometric methods (Bradburn, 1993, Coker, 1984, Stoloff, 1972). In this study, HPTLC was used for the detection and quantification of both AFB_1 and T-2 toxin.

4.1.2 HIGH PERFORMANCE THIN LAYER CHROMATOGRAPHY (HPTLC)

"High performance" TLC describes the range of techniques that have been used to improve the performance of conventional TLC; these are summarised in Table 43 and include sample extract application, densitometric quantification of the plate and the acquisition and processing of data by computer. This has led to better precision and accuracy and lower detection limits and consequently, HPTLC is now a viable alternative to HPLC for the determination of mycotoxins (Nawaz *et al.*, 1995; Bradburn, 1993; Ravindranath, 1989; Nesheim & Trucksess, 1986). Commercially available adsorbents for HPTLC include a precoated silica gel layer bound with 10-15% calcium sulphate or an organic polymer with a choice of glass, aluminium foil or acetate support (Ravindranath, 1989; Schmutz, 1980). The HPTLC sorbent layer, which is thinner and of a more uniform particle size than TLC layers (Table 45) allows faster separations over a shorter distance, reduced spot diffusion, better separation efficiency and lower detection limits (Ravindranath, 1989; Schmutz, 1980).

Method	TLC	HPTLC
Plate size	20x20	10x10
Layer thickness	100-250µm	200µm
Average particle size	20µm	2-15µm
Sample volume	1-5µl	0.1-0.2µl
Initial spot diameter	3-6mm	1.0-1.5mm
Final spot diameter	6-15mm	2-6mm
Solvent migration distance	10-15cm	3-6cm
Development time	30-200min	3-20min
Absorbance detection limit	1-5ng	0.1-0.5ng
Fluorescence detection limit	0.05-0.01ng	0.005-0.001ng
Samples per plate	10	18 or 36
Bradburn, 1993		

Table 45 Comparison of TLC and HPTLC.

4.1.2.1 Quantitative evaluation using HPTLC

In HPTLC, small volumes of sample extracts and analyte standards are applied to the sorbent. Up to 30 samples may be applied to one plate. Following chromatographic

separation, the amount of analyte in the extract is determined by densitometry. The difference between the optical signal from the sample-free background and that from the sample zone can be correlated with the concentration of the sample by comparison with the signal from standards of known concentration (Bradburn, 1993, Butler *et al.*, 1983).

Modern TLC densitometers mainly use reflectance measurements, as these offer certain advantages over transmission measurements. The usable spectral range is 800nm-200nm, irregularities in the layer, such as thickness, have less effect on the reflectance signal and light absorbing support materials, such as aluminium foils, can be used (Bradburn, 1993).

The analyte being measured must possess inherent optical properties, or be able to be derivatised into such a compound. Absorption or fluorescence measurements may be used. In absorption measurements the sample absorbs some of the incident radiation and the detector measures the decrease in the reflected radiation. Absorbance measurements often show a non-linear relationship between sample concentration and signal (peak area or height). With fluorescence measurements, part of the incident radiation is absorbed and emitted as lower energy radiation. This allows increased sensitivity and selectivity (Schmutz, 1980). A suitable filter, which blocks reflected light of the excitation wavelength but transmits fluorescent light, must be fitted between the sample and the photo detector. The relationship between signal and analyte concentration is linear over a wide concentration range, and sensitivity is 10-1000 times greater then that of absorbance measurements (Bradburn, 1993).

4.2 RESULTS AND DISCUSSION

4.2.1 SENSITIVITY OF *B. MEGATERIUM* TO AFLATOXIN B_1 AND T-2 TOXIN

The effect of AFB_1 (1µg/ml) and T-2 toxin (10µg/ml) on the growth of *B. megaterium* was determined as detailed in section 2.4.2.1, using an adaptation of the yeast bioassay methodology (section 2.3.1) and is shown in Figure 51; these toxin concentrations were used in the uptake experiments described later.

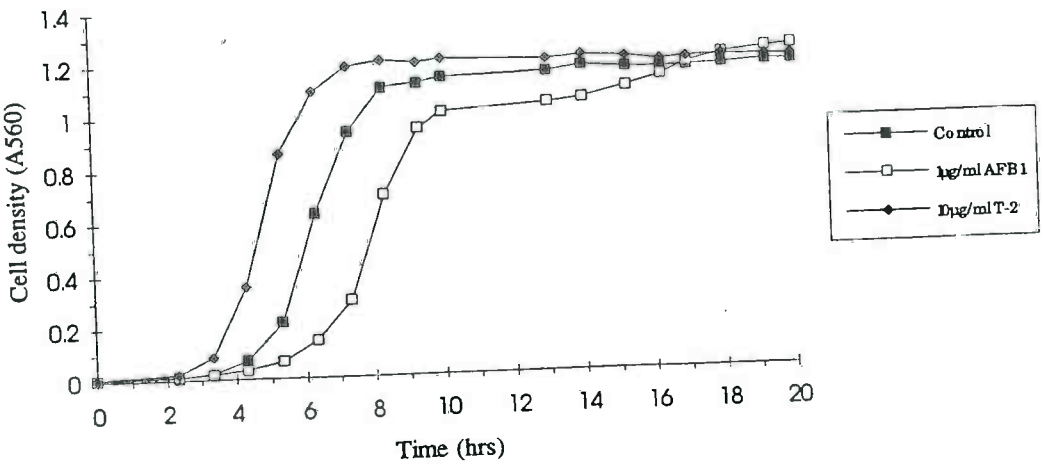

Figure 51 Effect of AFB_1 and T-2 toxin on the growth of *B. megaterium.*

1µg/ml AFB_1 (final concentration) had a slight inhibitory effect on growth of *B. megaterium* (Figure 51), however cells were able to recover from this, and final cell densities were similar to that of the control. Previous studies have shown the limits of detection of AFB_1 by *B. megaterium* to be 8µg/ml using inhibition of growth in a liquid culture assay (Tiwari *et al.*, 1985), 1µg/ml using inhibition of growth in a disk diffusion assay (Clements, 1968a,b, Jayaraman *et al.*, 1968) and 2µg/ml using inhibition of spore germination (Buckelew *et al.*, 1972).

In contrast, the presence of 10µg/ml T-2 toxin appeared to potentiate the growth of *B. megaterium*, relative to the control (Figure 51); growth in the presence of T-2 toxin being more rapid in the lag and log phases of growth, however, as for AFB_1 final cell densities were similar to the control.

Soil, water and rumenal bacteria have been shown to be capable of the deacylation of T-2 toxin and can use it as sole carbon and energy source (Ueno *et al.*, 1983b; Beeton & Bull, 1989, Swanson *et al.*, 1988), furthermore, deacylation produces metabolites that have a reduced toxicity relative to the parent toxin (see section 1.2.2.3). It may be that *B. megaterium* is capable of the deacylation of T-2 toxin, and the metabolites produced are non-toxic and act in some way to potentiate the growth of this bacterium.

4.2.2 UPTAKE AND BINDING OF AFLATOXIN B_1 BY *K. MARXIANUS*

4.2.2.1 Precision of the methodology

The precision of the methodology for determining the uptake and binding of AFB_1 by *K. marxianus* was determined as detailed in section 2.4.2.2.1, using three replicate samples. Cultures were incubated with 5µg of AFB_1 for 16 hours at 37°C, after which the amount of AFB_1 in extracts of the supernatant, washes and ruptured cells was determined.

The amount of AFB_1 (ng) in the various extracts from the three replicates is shown in Table 46; the percentage of AFB_1 in each extract was calculated using equation 7 (page 93) and is also shown in Table 46. Mean ($\bar{x}$), standard deviations (s.d.) and coefficients of variation (% CV) were calculated for each group of replicates and are also given.

As can be seen from Table 46, the precision of the procedure was found to be good. Standard deviations for replicate extracts were found to be low, and % CV were below 10% for all replicates and below 5% for most replicates; the higher % CV were generally being found for replicates containg very low levels of AFB_1 (Table 46). The overall recovery of AFB_1 was excellent, with 100% recovery for all replicates.

cells were exposed (calculated using equation 7, page 93) and the latter is shown in Figure 52.

Cell density at the end of the 16 hour incubation period was determined, using a haemocytometer, and is shown in Table 48. This measurement was used to determine the amount of AFB_1 (ng) associated with each cell (also shown in Table 48).

HPTLC plates were examined for the production of metabolites of AFB_1 by *K. marxianus* as detailed in section 2.4.1.6.4. No metabolites of AFB_1 were detected in any of the sample extracts.

Methanol	0%	0%	5%	8.5%	15%
PMBS	0	15µg/ml	15µg/ml	15µg/ml	15µg/ml
AFB_1 in each fraction (ng)					
Supernatant	4180.04	3812.88	3775.71	4069.77	4092.86
Wash (1-5)	673.86	674.91	659.36	563.50	523.19
Ruptured cells	28.39	24.79	26.17	17.84	13.30
% AFB_1 in each fraction					
Supernatant	84	84	83	92	90
Wash (1-5)	14	15	14	13	11
Ruptured cells	0.57	0.54	0.57	0.40	0.29
Recovery (%)	98	99	98	102	101

Table 47 Effect of methanol and PMBS on the uptake and binding of AFB_1 by *K. marxianus* as determined following the exposure of 5ml cultures to 5µg of AFB_1 for 16 hours at 35°C.

Methanol	0%	0%	5%	8.5%	15%
PMBS	0	15µg/ml	15µg/ml	15µg/ml	15µg/ml
Amount of AFB_1 associated with each cell (ng)					
No. cells/ml	3.65×10^8	3.60×10^8	3.55×10^8	2.69×10^8	2.14×10^8
AFB_1/cell (ng)	1.56×10^{-8}	1.38×10^{-8}	1.47×10^{-8}	1.33×10^{-8}	1.24×10^{-8}

Table 48 Effect of methanol and PMBS on growth of *K. marxianus* and the amount of AFB_1 associated with the cells.

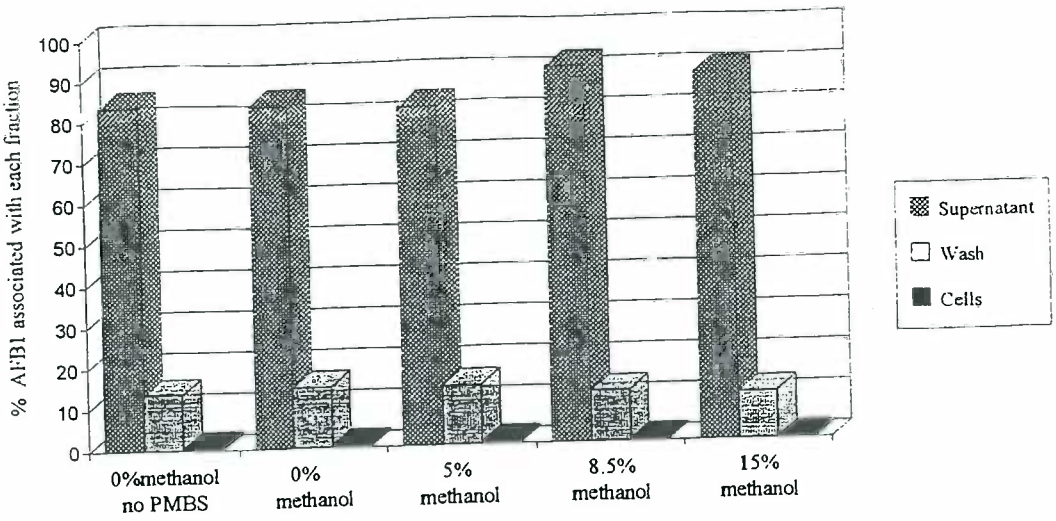

Figure 52 Effect of methanol and PMBS on the uptake and binding of AFB_1 by *K. marxianus*: percentage of AFB_1 associated with each fraction. Cultures contained various amounts of methanol as stated on the graph and were supplemented with 15µg/ml PMBS unless otherwise stated.

The data shown in Table 47 and Figure 52 clearly shows that under all conditions tested, the majority of AFB_1 (83-92%) was found in the supernatant extract; this being toxin not associated in any way with the yeast cells. A smaller amount (a total of 11-15%) was detected in the extracts from the wash solutions, and the amount of toxin in a given wash extract was found to decrease with increasing number of washes (see Table 3a Appendix 3); this is toxin that is losely bound to the outside of the yeast cells. Only a very small amount (0.3-0.6% or 13-26ng) was found in the extracts from the ruptured cells, and is toxin that is inside the cells.

The presence of PMBS had no significant effect on the uptake of AFB_1 by *K. marxianus* (Table 47 and Figure 52), the proportion of AFB_1 in extracts from the supernatant, wash and ruptured cells being very similar in the presence and absence of PMBS.

Methanol appeared to elicit an increase in the amount of AFB_1 in the supernatant extract and a decrease in the amount of AFB_1 in the combined washes and the

ruptured cell extracts at concentrations of 8.5 and 15% (v/v) (Table 47 and Figure 52); earlier in this thesis, the toxicity of methanol to *K. marxianus* was reported (section 3.1.5), and as can be seen in Table 48, in the experiments reported here methanol also caused a significant inhibition of growth at 8.5 and 15% (v/v). The amount of AFB_1 associated with the ruptured cells was therefore expressed as a function of cell density (Table 48) and when final cell density was taken into account it was found that the amount of AFB_1 associated with the cells was fairly similar for all conditions tested (Table 48).

It therefore appears that rather than inhibiting the uptake and binding of AFB_1 by *K. marxianus,* methanol inhibited the growth of *K. marxianus,* with the consequence that at higher methanol concentrations there were fewer cells present to take up AFB_1, leading to the apparently lower levels of AFB_1 seen at the higher methanol concentrations (Table 47 and Figure 52).

In conclusion, neither methanol or PMBS appeared to have a significant effect on the uptake and binding of AFB_1 by *K. marxianus.* However, at 8.5 and 15% (v/v) methanol was toxic to *K. marxianus* and caused a significant inhibition of growth.

4.2.3 UPTAKE AND BINDING OF AFLATOXIN B_1 BY *B. MEGATERIUM*

4.2.3.1 Precision of the methodology

The precision of the methodology was determined as detailed in section 2.4.2.3.1, using three replicate samples; cultures were incubated with 5µg of AFB_1 for 16 hours at 37°C, after which the amount of AFB_1 in extracts of the supernatant, washes and ruptured cells was determined.

The amount of AFB_1 (ng) in the various extracts from the three replicates is shown in Table 48; the percentage of AFB_1 in each extract was calculated using equation 7 (page 93) and is also shown in Table 49. Mean ($\bar{x}$), standard deviations (s.d.) and coefficients of variation (% CV) were calculated for each group of replicates and are also given.

Extract	Replicate 1	Replicate 2	Replicate 3	$\bar{x}$	s.d.	%CV
	AFB_1 in each extract (ng)					
Supernatant	3145.41	3225.00	3175.73	3182.05	32.80	1.03
Wash 1	484.11	505.46	491.33	493.63	8.87	1.80
Wash 2	103.25	123.48	116.13	114.29	8.36	7.32
Wash 3	29.67	35.87	30.40	31.98	2.77	8.65
Wash 4	8.25	8.13	9.75	8.71	0.74	8.46
Wash 5	2.02	1.76	1.69	1.82	0.14	7.79
Cells	6.51	8.26	7.27	7.35	0.72	9.75
Total	3779.22	3907.96	3832.30	3839.83	52.83	1.68
	Percentage of AFB_1 in each extract					
Supernatant	71.78	73.59	72.47	72.61	0.92	1.26
Wash 1	11.05	11.53	11.21	11.26	0.25	2.20
Wash 2	2.36	2.82	2.65	2.61	0.23	8.96
Wash 3	0.68	0.82	0.69	0.73	0.08	10.60
Wash 4	0.19	0.19	0.22	0.20	0.02	10.36
Wash 5	0.05	0.04	0.04	0.04	0.00	9.54
Cells	0.15	0.19	0.17	0.17	0.02	11.94
Recovery (%)	86	89	87	87	1.21	1.68

Table 49 Precision of procedure for determining uptake and binding of AFB_1 by *B. megaterium.*

The precision of procedure was good, showing both low standard deviations and coefficients of variation (Table 49); however, the total recovery was less than 90%, this contrasting markedly with the results for *K. marxianus*, for which recovery was 100% (section 4.2.3.1). This lower level of recovery was however repeatable and it was felt that the methodology was sufficiently precise and accurate to be used in the determination of the effect of methanol on the uptake and binding of AFB_1 by *B. megaterium.*

4.2.3.2 Effect of methanol on the uptake and binding of AFB_1 by *B. megaterium*

The effect of methanol on the uptake and binding of AFB_1 by *B. megaterium* was determined as detailed in section 2.4.2.3.2; cultures were incubated with 5µg of AFB_1 for 16 hours at 37°C, after which the amount of AFB_1 in extracts of the supernatant, washes and ruptured cells was determined.

The effect of methanol on the uptake and binding of AFB_1 by *B. megaterium* is summarised in Table 50 below, and a full breakdown of the results is given in Table

3b in Appendix 3. In both tables, the amount of AFB_1 (ng) found in each extract is given, this is also expressed as a percentage of total AFB_1 to which the cells were exposed (calculated using equation 7, page 93) and the latter is shown in Figure 53. Cell density at the end of the 16 hour incubation period was determined, using a haemocytometer, and is shown in Table 51. This reading was used to determine the amount of AFB_1 (ng) associated with each cell (which is also given in Table 51). HPTLC plates were examined for the production of metabolites of AFB_1 as detailed in section 2.4.1.6.4. No metabolites of AFB_1 were detected in any of the sample extracts.

Methanol	0%	5%	8.5%	15%
AFB_1 in each fraction (ng)				
Supernatant	3230.04	3379.84	3348.97	3301.94
Wash	644.51	600.49	561.54	521.68
Cells	7.29	11.06	13.90	11.92
% AFB_1 in each fraction				
Supernatant	73	75	75	74
Wash	15	13	13	12
Cells	0.16	0.25	0.31	0.27
Recovery (%)	88	89	88	86

Table 50 Effect of methanol on the uptake and binding of AFB_1 by *B. megaterium* as determined following the exposure of 5ml cultures to 5µg of AFB_1 for 16 hours at 35°C.

Methanol	0%	5%	8.5%	15%
Amount of AFB_1 associated with each cell (ng)				
No. cells/ml	3.48×10^{8}	2.98×10^{8}	2.15×10^{8}	1.90×10^{8}
AFB_1/cell	4.19×10^{-9}	7.42×10^{-9}	1.29×10^{-8}	1.25×10^{-8}

Table 51 Effect of methanol growth of *B. megaterium* and the amount of AFB_1 associated with the cells

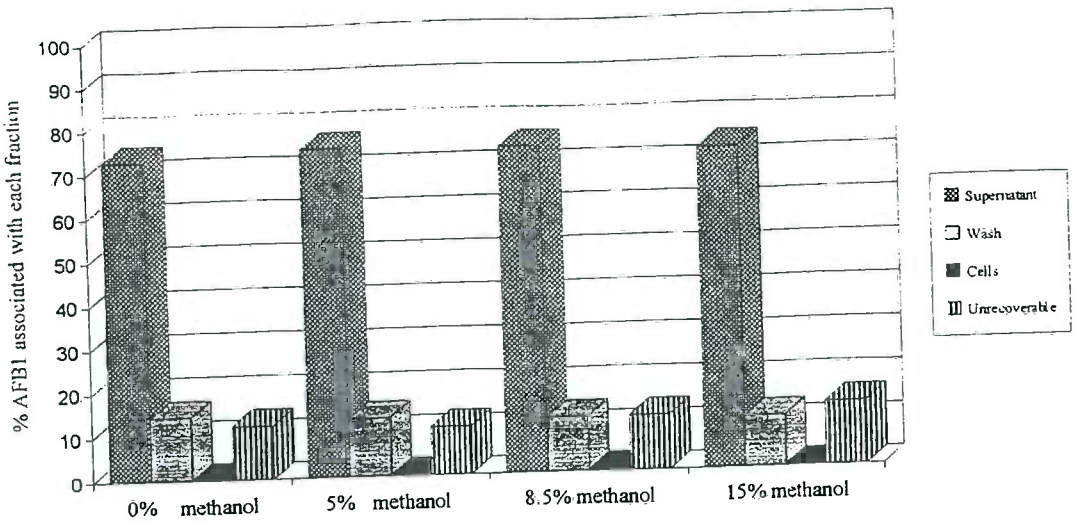

Figure 53 Uptake and binding of AFB_1 by *B. megaterium*. Percentage of AFB_1 associated with each fraction.

As with *K. marxianus*, the majority (73-75%) of AFB_1 was found in the supernatant extract and was not associated with the bacterial cells (Table 50 and Figure 53); however, the amount of AFB_1 in the supernatant extract from *B. megaterium* was approximately 10% less than that for *K. marxianus* (Table 48) and this was reflected in the final percentage recovery, which was approximately 90% for *B. megaterium* (Table 50) compared to 100% for *K. marxianus* (Table 47). A smaller amount (12-15%) was found in the extracts from the wash solutions, which is similar to the value obtained for *K. marxianus*. Only a very small amount of toxin (0.16-0.31% or 7-14ng) was found in the extract from the ruptured cells (Table 50 and Figure 53), which again is similar to that obtained using *K. marxianus* (Table 47 and Figure 53).

As with *K. marxianus*, increasing methanol concentrations had an inhibitory effect on the growth of *B. megaterium*, (Table 51) growth being inhibited to some extent at all methanol concentrations tested. Despite this inhibition of growth, the presence of methanol had a small but possibly significant effect on the uptake and/or binding of AFB_1 by *B. megaterium*, this being seen from both absolute values (Table 50) and when the uptake of AFB_1 was expressed in terms of cell density (Table 51). This

observation is in contrast to *K. marxianus* in which methanol had no effect on the uptake and/or binding of AFB_1 when expressed in terms of cell density (Table 48). In *B. megaterium*, methanol therefore appears to potentiate uptake of extractable AFB_1 this being maximal at 8.5% (v/v) methanol and may be due to methanol-induced increased membrane permeability.

The recovery of AFB_1 from extracts of *B. megaterium* cultures was found to be approximately 90% (at all methanol concentrations tested). This contrasts with *K. marxianus* extracts for which the recovery was 100% and may indicate that metabolism of AFB_1 occurs in *B. megaterium* and not *K. marxianus*. This is quite plausable, since AFB_1 is toxic to *B. megaterium* and not to *K. marxianus* (Figure 51), and toxicity is known to require metabolic acitivation by cyt P450 (see section 1.2.1.4). However, on examination of the HPTLC plates, no metabolites of AFB_1 were found in the extracts from either *K. marxianus* or *B. megaterium*. A possible explanation may be that about 10% of the AFB_1 becomes irreversibly bound to components of the *B. megaterium* cells, (perhaps after metabolic alteration) and as such would not be extractable and therefore not detectable on the HPTLC plates. Furthermore, assuming metabolic activation does occur, polar, water-soluble metabolites may be produced, which are not readily partitioned from aqueous homogenates using chloroform (Swanson & Corley, 1989) and again these would not be detectable on the HPTLC plates.

4.2.4 UPTAKE AND BINDING OF T-2 TOXIN

The methodology for the detection of AFB_1 by HPTLC is well established and it is known there is a linear relationship between AFB_1 concentration in the sample and detector response (peak area) (Nawaz *et al.*, 1995). However for T-2 toxin the methodology is less well characterised, and the relationship between sample concentration and detector response was assessed to ensure it was linear.

4.2.4.1 Detection of T-2 toxin by HPTLC

The relationship between the concentration of T-2 toxin in each sample and the detector-response (peak area) was determined as detailed in section 2.4.2.4 and is shown in Figure 54.

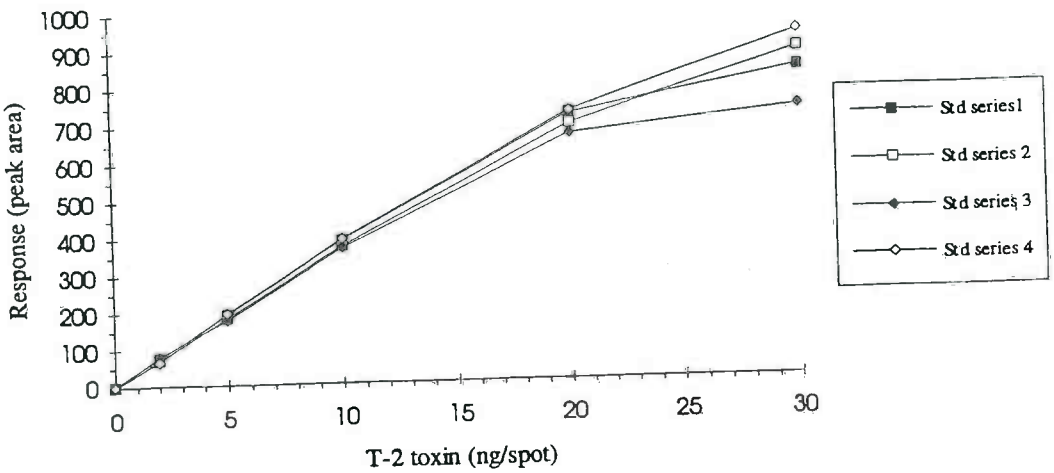

Figure 54 Linearity of detection of T-2 toxin using HPTLC

The sample concentration-detector response relationship was essentially linear up to a concentration of 20ng/spot, but deviated significantly thereafter (Figure 54). The maximum amount of T-2 in any sample would be <10µg/ml - cultures were spiked with 50µg of T-2 toxin; if all the T-2 toxin was recovered in one extract that was diluted in 5ml of B:A this would give a concentration of 10µg/ml, which when spotted on the plate gives a spot concentration of 20ng. Therefore, samples to be analysed in this study would all contain toxin concentrations which show a linear relationship with detector-response, and the estimation of T-2 in each sample was therefore made using equation 7 (page 93) and not using of a calibration curve which is necessary if the relationship is non-linear.

4.2.4.2 Uptake and binding of T-2 by *K. marxianus* and *B. megaterium*

Since methanol was shown not to have large effects on the uptake of AFB_1 by either *K. marxianus* or *B. megaterium*, the uptake of T-2 toxin in the presence of 5% methanol only was examined as detailed in section 2.4.2.5; cultures were incubated with 50µg of T-2 toxin for 16 hours at 37°C, afterwhich the amount of T-2 toxin in extracts of the supernatant, washes and ruptured cells was determined.

The uptake and binding of T-2 toxin by *K. marxianus* and *B. megaterium* is summarised in Table 52, below, and a full breakdown of the results is given in Table 3c in Appendix 3. In both tables, the amount of T-2 toxin (µg) found in each extract is given, and is also expressed as a percentage of total T-2 toxin to which the cells were exposed (calculated using equation 7, page 93).

HPTLC plates were examined for the production of metabolites of T-2 toxin by both microorganisms as detailed in section 2.4.1.7.4. No metabolites of T-2 toxin were found in any of the sample extracts.

The uptake of T-2 toxin and AFB_1 by *K. marxianus* and *B. megaterium* is directly compared in Figure 55.

Organism	*K. marxianus*	*B. megaterium*
Sample	Percentage of T-2 toxin associated with each fraction	
Supernatant	96	84
Wash	7	8
Cells	0.02	0.02
Recovery (%)	102	92

Table 52 Uptake and binding of T-2 toxin by *K. marxianus* and *B. megaterium*. Percentage of T-2 toxin associated with each fraction

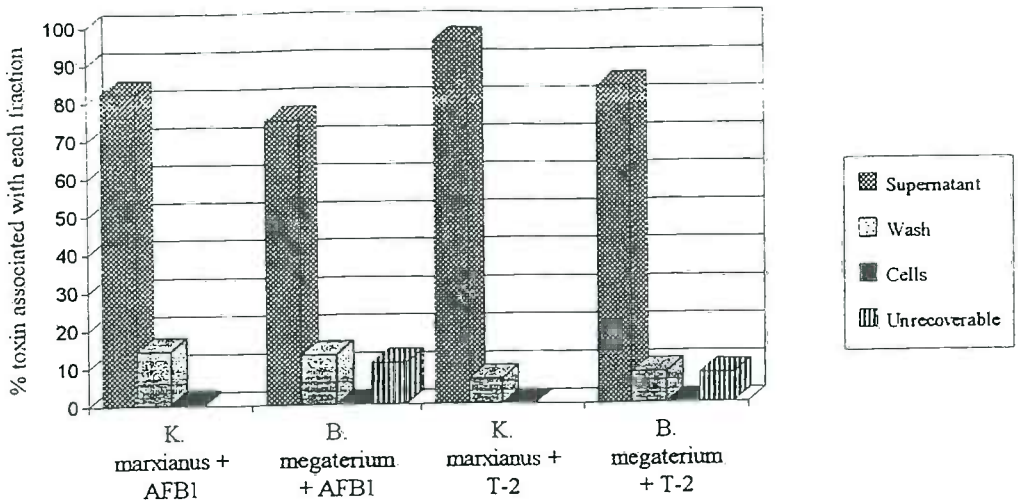

Figure 55 Uptake of AFB_1 and T-2 toxin by *K. marxianus* and *B. megaterium* in the presence of 5% methanol

The results for the uptake and binding of T-2 toxin by *K. marxianus* and *B. megaterium* were comparble to those reported earlier, using AFB_1.

For both microorganisms the majority of T-2 toxin (96% for *K. marxianus* and 84% for *B. megaterium*) was found in the supernatant extract and was not associated with the cells; a smaller amount was detected in the combined wash solutions (7% for *K. marxianus* and 8% for *B. megaterium*). Only a very small amount (0.02% or 10ng for both microoganisms) was found in the ruptured cells extract (Table 52); in the case of *K. marxianus* this small quantity of T-2 taken up is sufficient to be highly toxic, whereas in *B. megaterium*, in is non-toxic and may actually potentiate growth (Figure 51, section 4.2.1).

Interestingly, once again, toxin recovery from *B. megaterium* was incomplete. This may indicate the metabolism of T-2 toxin by *B. megaterium* and not *K. marxianus*, and the permanent sequestering of T-2 metabolites, (or a proportion of the T-2 itself), by the bacterial cells.

4.3 CONCLUSIONS

The uptake experiments with both toxins (AFB_1 and T-2 toxin) and both microorganisms show a broadly similar pattern: the great majority of the toxin was found in the supernatant and wash fractions, and only very small amounts of toxin (<0.5% of total used in each experiment) were recoverable from the ruptured cells. However, these small amounts of toxins elicited very different effects in the two microorganisms. In *K. marxianus,* T-2 toxin (≥100ng/ml) caused the complete inhibition of growth (Figure 2c, page 223), whereas AFB_1 (≥1μg/ml) was non-toxic and had no inhibitory effect on growth (Table 43, page 139); in contrast, in *B. megaterium,* T-2 toxin (10μg/ml) was non-toxic and appeared to potentiate growth, whereas AFB_1 (1μg/ml) caused a slight inhibition of growth (Figure 51, page 156). The lack of sensitivity of *K. marxianus* to AFB_1, reported earlier in this thesis (section 3.2.2, page 139), therefore does not appear to be due solely to the lack of toxin entry into the yeast cells.

Interestingly, approximately 10% of both toxins was found to be non-recoverable from the *B. megaterium* culture, whereas toxin recoveries from cultures of *K. marxianus* were 100%. This may suggest irreversible binding of the toxin material to *B. megaterium* cells and is consistent with metabolic alterations/activation of the toxins so that they bind firmly, (probably covalently) to cell structures. Metabolism of mycotoxins is mediated by cyt P450, and *B. megaterium* is known to contain an active cyt P450 system (Narhi & Fulco, 1987), which may be involved in the metabolism of AFB_1 and T-2 toxin. Furthermore, an insufficiency, or a lack of cyt P450 in *K. marxianus* may account for both lack of sensitivity of this yeast to AFB_1 and the high level of sensitivity to T-2 toxin and other trichothecene mycotoxins. Metabolic activation (by cyt P450) is a requisite step in the toxigenicity of AFB_1 whereas metabolism of the trichothecenes produces less toxic metabolites, therefore in the absence of cyt P450, AFB_1 would remain non-toxic whereas the more toxic parent trichothecenes would persist. The presence of an active cyt P450 in *K. marxianus*, strain C25, (from the Technical Research Centre, Finland) has been

reported (Karenlampi *et al.*, 1980); however, the metabolic capabilities of *K. marxianus* (GK1005) are unknown, and in view of this, levels of cyt P450 in *K. marxianus* (GK1005) were determined and its ability to bind AFB_1 examined, and are discussed in Chapter 5.

PMBS and methanol had no effect on the uptake and binding of AFB_1 by *K. marxianus*, but at 8.5 and 15% (v/v) did inhibit growth. In *B. megaterium,* methanol inhibited growth to some extent at all concentrations tested (5, 8.5 and 15% (v/v)), and in contrast to *K. marxianus*, potentiated the uptake of AFB_1 by the bacterial cells.

The sensitivity and the range of detection of mycotoxins by *K. marxianus* was found to vary considerably when using the Bioscreen assay (developed by Dell, 1993) and the colorimetric microtitre plate assay (developed in this thesis) and was discussed earlier (page 140). One factor thought to be involved was the different methanol concentrations used in the two assays (8.5% (v/v) in the Bioscreen bioassay and 5% (v/v) in the microtitre plate assay). However, the results reported here show that the uptake of AFB_1 by *K. marxianus* is not potentiated by methanol, and differences in the methanol concentration does not appear to account for the differences in detection and sensitivity of the two assays; the cause of the enhanced sensitivity and range of detection of mycotoxins seen in the Bioscreen assay by Dell (1993) remains unresolved.

CHAPTER 5

CHARACTERISATION OF CYTOCHROME P450 OF *K. MARXIANUS*

5.1 INTRODUCTION

5.1.1 OBJECTIVES

The insensitivity of *K. marxianus* (GK1005) to non-trichothecene mycotoxins, such as aflatoxin B_1, does not appear to be due to the lack of uptake and entry into the yeast cells. As discussed in Chapter 4, small, but similar amounts of T-2 toxin and AFB_1 were recoverable from the ruptured yeast cells, but were found to elicit very different effects on the growth of *K. marxianus;* T-2 toxin was found to be very toxic and completely inhibited growth, (at concentrations as low as 100ng/ml), whereas AFB_1 was non-toxic and had no detectable effect on growth, even at very high concentrations (25μg/ml). An alternative reason for the insensitivity of *K. marxianus* to AFB_1 may be the lack or insufficiency of an appropriate (cyt P450) activating system. To further clarify this issue it was decided to determine the levels of cyt P450 in microsomal samples from *K. marxianus*, and examine the binding of AFB_1 by these cytochromes. For control purposes, similar experiments were performed using *Saccharomyces cerevisiae* (NCYC 754), which has been reported to contain high levels of cyt P450 (King *et al.,* 1985; King *et al.*, 1983b), and benzo(*a*)pyrene, a known substrate of cyt P450 in *S. cerevisiae* (Kelly & Kelly, 1988; Kelly *et al.,* 1985; King *et al.*, 1983b; Wiseman & Woods, 1979).

5.1.2 CYTOCHROMES P450

Cytochromes P450, (cyt P450), is the generic name for a group of haem-containing enzymes found in a wide variety of organisms, ranging from bacteria to humans. They derive their name from their characteristic reduced carbon monoxide difference spectrum, which has a spectral peak at about 450nm. Cyt P450 catalyse a wide range of reactions including the monooxygenation of xenobiotic compounds, such as drugs, pesticides and carcinogens, as well as endogenous compounds, such as fatty acids and sterols (Sato & Omura, 1978). Cyt P450 can act as oxidases, peroxidases or reductases and can catalyse aliphatic and aromatic hydroxylation, epoxidation, N-, O- and S-dealkylation, deamination, sulphoxidation and dehalogenation reactions (Schenkman, 1991). However, their most common activity is as the terminal oxidase

in stereo-specific mono-oxygenase reactions. This reaction can be represented simply as:-

$$SH + NADPH + H^+ + O_2 \longrightarrow SOH + NADP^+ + H_2O$$

where SH is the substrate and SOH the product.

Cyt P450 require the presence of other microsomal enzymes for normal monooxygenase activity. These include a membrane-bound flavoprotein (containing both flavin adenine dinucleotide (FAD) and flavin mononucleotide (FMN)) and NADPH-cyt P450 reductase, or in the case of some cyt P450-mediated reactions, (particularly fatty acid and sterol metabolism), cytochrome b_5 and cytochrome b_5 reductase (Lee & Snyder, 1973). In contrast, mitochondrial and bacterial cyt P450 are associated with a flavoprotein (containing FAD) and an iron-sulphur protein (Omuro *et al.*, 1966); the bacterial and mitochondrial systems differ in that the former is soluble, and not membrane-bound.

The organisation and function of the eukaryotic microsomal system has been studied predominantly in relation to the metabolism of foreign compounds in the liver. Cytochromes P450 perform phase I reactions on lipophilic substrates, introducing polar groups onto the substrate molecule.

Eukaryotic microsomal cyt P450 are present in lower eukaryotes, including yeast, and were first demonstrated in *Saccharomyces cerevisiae* by Lindenmayer & Smith (1964); they have since been demonstrated in several other species including a strain of *K. marxianus* (Karenlampi *et al.*, 1980). The cyt P450 reduced carbon monoxide difference spectrum of *S. cerevisiae* shows an absorption maximum at 448nm; the physiological role of this cyt P450 is in the biosynthesis of ergosterol, a major sterol of the yeast cell membrane (Alexander *et al.*, 1974). The yeast system resembles the mammalian system with a cytochrome P450 haemoprotein coupled to a NADPH-cyt P450 reductase in the microsomal fraction. Two forms of cyt P450 appear to be involved in ergosterol biosynthesis (Kappeli, 1986): cyt $P450_{14\text{-}DM}$ is involved in the C-14 demethylation of lanosterol (Aoyama *et al.*, 1984, 1987); and a second, minor

form, cyt $P450_{22\text{-}DS}$, is thought to perform the Δ^{22}-desaturation step of ergosterol biosynthesis (Hata *et al.*, 1987, 1983). In other yeast species, such as *Candida tropicalis*, other forms of cyt P450 (cyt $P450_{alk}$) are involved in the initial metabolism of alkanes (Sanglard *et al.*, 1986).

The affinity of cyt P450 for substrates can be investigated using analysis of substrate-induced spectral shifts. Upon substrate binding, the cytochrome shifts from low-spin to high-spin form and this is characterised by an absorbtion peak at 390nm and a dip at about 420nm, and is termed type I binding (Jefcoate, 1979). Inhibitors such as primary amines and azole-base fungicides induce the type II binding spectrum, which is characterised by a peak at 425-430nm and a minimum at 390-410nm (Jefcoate, 1979). A reverse-type I spectral change has also been reported, which is the mirror image of the type I spectum, and has an absorbtion maximum at approximately 420nm and a minimum at about 385nm.

Since type I compounds are almost invariably substrates for cyt P450, the type I spectral change reflects the formation of a true enzyme-substrate complex beween cyt P450 and the substrate (Jefcoate, 1979), and difference spectroscopy can therefore be used to determine the extent and mode of substrate binding with cyt P450. Schenkman *et al.* (1967) showed that the spectral dissociation constant, (K_S), - the substrate concentration required for half-maximal spectral change - can be a useful measure of the enzyme's affinity for the substrate, and can be calculated from the binding spectra (see section 2.5.5, page 99).

The cyt P450 of *S. cerevisiae* have been shown to have a broad substrate range, and can hydroxylate benzo(*a*)pyrene (B(*a*)P) (Wiseman & Woods, 1979) and metabolise several promutagens, including aflatoxin B_1 (Callen & Philpot, 1977; Callen *et al.*, 1980; Kelly & Parry, 1983; Niggli *et al.*, 1986). The metabolism of B(*a*)P by *S. cerevisiae* is catalysed by a form of cyt P450 other than cyt $P450_{14\text{-}DM}$, (Kelly *et al.*, 1993) and the metabolic profile of B(*a*)P metabolism by yeast microsome is similar to that generated by mammalian P-448 (King & Wiseman, 1987). Cyt P450 from

S. cerevisiae shows a reduced affinity for benzo(*a*)pyrene compared to rat liver microsomes (Kelly *et al.*,1985; Kelly & Kelly, 1988).

5.2 RESULTS AND DISCUSSION

5.2.1 CARBON MONOXIDE DIFFERENCE SPECTRA

Reduced carbon monoxide spectra were investigated for microsomal samples from *K. marxianus* (GK1005) and as a control, *S. cerevisiae* (NCYC 754), as detailed in section 2.5.3, and are shown in Figures 56 and 57, respectively.

As expected, the microsomal fraction of *S. cerevisiae* exhibited a reduced carbon monoxide spectrum typical of cyt P450, (Figure 56); it showed an absorbance peak at 451nm, and contained 32±8 pmol of cyt P450 per mg protein (average of three experiments). A small shoulder was also discernible at 427nm, and is probably caused by cyt P420, a breakdown product of cyt P450.

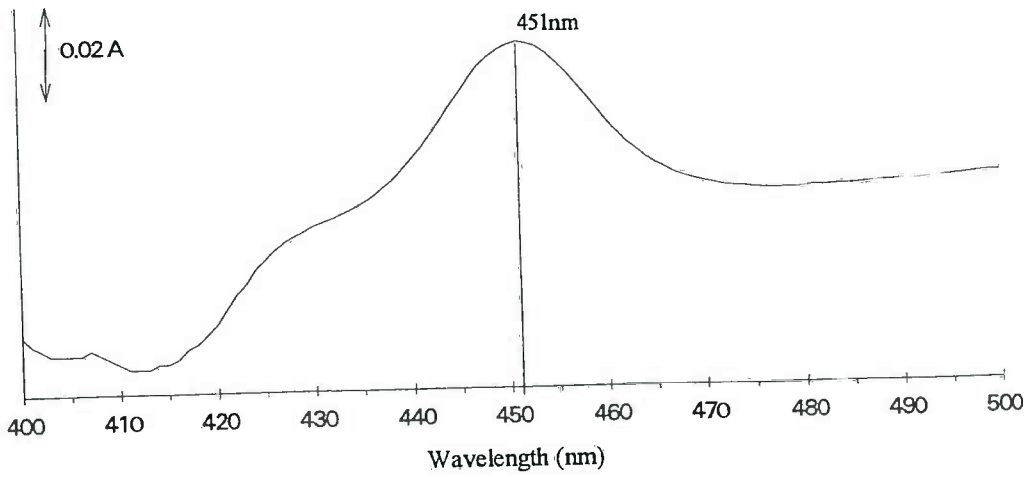

Figure 56 Typical reduced carbon monoxide difference spectrum obtained with a microsomal fraction of *S. cerevisiae*, NCYC 754.

Levels of cyt P450 in the microsomal fraction of *S. cerevisiae* (NCYC 754) were lower than those previously reported by King *et al.*, (1985), who found levels of 85 pmol of cyt P450 per mg protein; a direct comparison with other literature reports (King *et al.*,

1983b, Karenlampi, 1980) was not possible, as these express cyt P450 content as pmol per gram wet weight of whole cells , rather than per mg protein.

The peak at 451nm shows a shift of 3nm from values in the literature, which agree on a peak at 448nm for this particular strain (King *et al.*, 1985) and for *S. cerevisiae* strains JL10 (Yoshida & Aoyama, 1984) and JL745 (Kalb *et al.*, 1986). This disparity between values reported here and the literature values may be due to the contamination of samples with other carbon monoxide-binding pigments. Gross contamination by mitochondrial cytochrome c oxidase, which has a spectral minimum at 445nm and absorbs strongly at 428m, has been reported to mask the reduced carbon monoxide difference spectrum of cyt P450, whereas more mild contamination has been reported to cause unusual peaks (Kapelli *et al.*, 1982; Karenlampi *et al.*, 1980); however, the largest effect might be expected to derive from cytochrome a_3, which causes a negative peak at around 440nm in the reduced carbon monoxide spectrum (Ishidate *et al.*, 1969; Lindenmayer & Smith, 1964). Contamination of the microsomal fraction with mitochondrial carbon monoxide-binding pigments seems to be the most likely cause of the shift in the peak, shown in Figure 56; this problem may be avoided by the use a more gentle method for microsome preparation, such as speroplast preparation followed by mild mechanical disruption or osmotic shock and the precipitation of the microsomes using calcium chloride (Kapelli, 1986).

In contrast to *S. cerevisiae,* the microsomal fraction from *K. marxianus* did not exhibit a reduced carbon monoxide spectra (Figure 57). This result differs from the findings of a previous study in which whole cell suspensions of a strain of *K. marxianus,* (strain C25, from the Technical Research Centre, Finland) showed a reduced carbon monoxide difference spectrum typical of cyt P450 (Karenlampi *et al.*, 1980); the absorbance maximum was found to occur at 451nm, and the cells contained 1.87nmol cyt P450 per g wet weight of cells. In the same study, *S. cerevisiae* (NCYC 240) showed an absorbance peak at 448nm and contained 4.66nmol cyt P450 per g wet weight of cells.

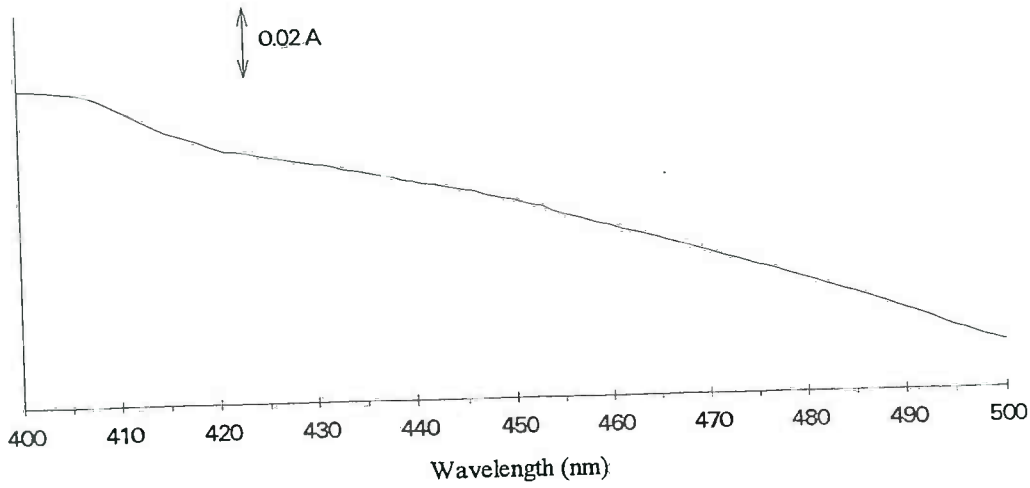

Figure 57 Typical reduced carbon monoxide difference spectrum obtained with the microsomal fraction of *K. marxianus*, GK1005.

It would be most unusual for a yeast not to contain cyt P450, as it plays an essential role in the biosynthesis of ergosterol, a major sterol of yeast membranes (Alexander *et al.*, 1974; Aoyama *et al.*, 1984, 1987; Hata *et al.*, 1987). It therefore seems unlikely that there is a complete absence of cyt P450 in *K. marxianus* (GK1005), and more likely that levels of cyt P450 in this yeast strain were below the limits of detection of the method used and/or that the microsomal fraction was contaminated by mitochondrial carbon monoxide-binding pigments which masked the cyt P450 reduced carbon monoxide difference spectra; this hypothesis is further supported by the results of the substrate binding studies.

5.2.2 SUBSTRATE BINDING SPECTRA

The binding of two substrates, benzo(*a*)pyrene (B(*a*)P) and aflatoxin B_1 (AFB_1) to microsomal samples from *S. cerevisiae* and *K. marxianus* was determined as detailed in section 2.5.5.

5.2.2.1 Benzo(*a*)pyrene binding spectra

A spectral change was observed upon the addition of benzo(*a*)pyrene (B(*a*)P) to microsomal samples from both *S. cerevisiae* and *K. marxianus*, resulting in a typical Type I binding spectra, with maxima at 392nm and minima at 420nm (see Figures 58 and 62). Second peaks were also observed at 371nm, comparable to the additional, 367nm, peak noted by Kelly *et al.*, (1993).

Spectral titration was used to calculate K_S values from Lineweaver-Burk, Eadie-Hofstee and Hanes plots using equations 10, 11 & 12, (page 100), respectively; and are shown in Figures 59, 60 and 61 for *S. cerevisiae* and Figures 63, 64 and 65 for *K. marxianus*. K_S values obtained from each type of plot are shown in Table 53; the mean K_S values for the binding of B(*a*)P to microsomal cyt P450 from *S. cerevisiae* and *K. marxianus* were found to be 70μM and 82μM respectively; and were found not to differ significantly using the t-test.

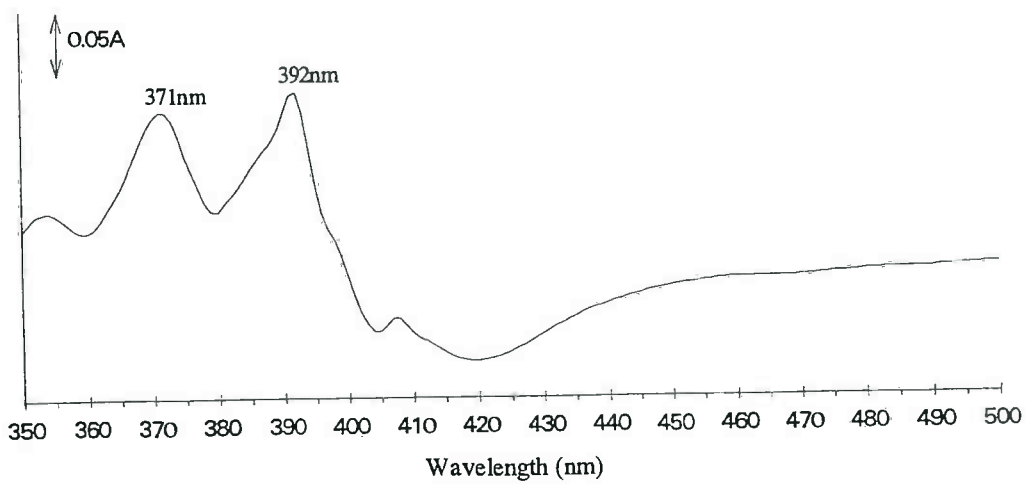

Figure 58 Type I substrate binding on the addition of 10μg/ml benzo(*a*)pyrene to microsomal cyt P450 from *S. cerevisiae*.

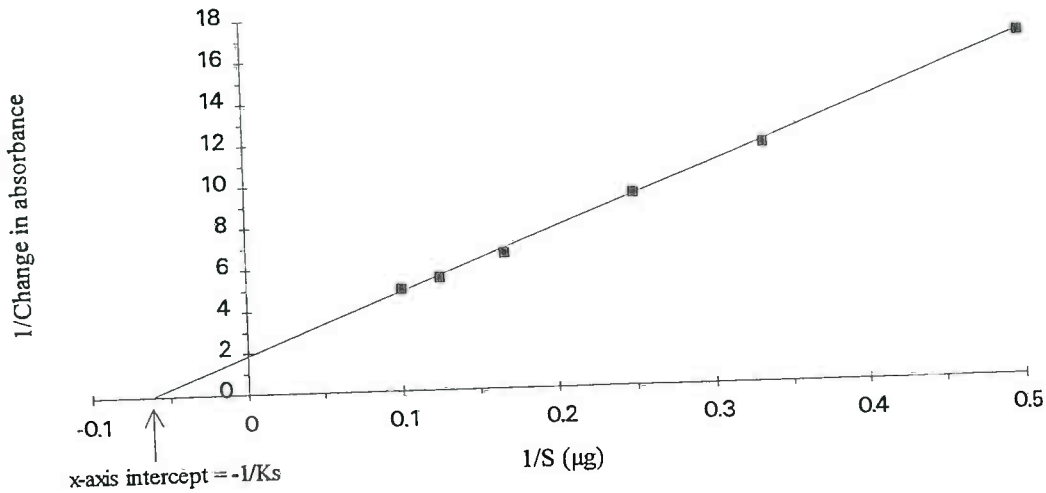

Figure 59 Lineweaver-Burk plot for the binding of benzo(*a*)pyrene with microsomal P450 from *S. cerevisiae*. (1/S = 1/substrate concentration (µg)).

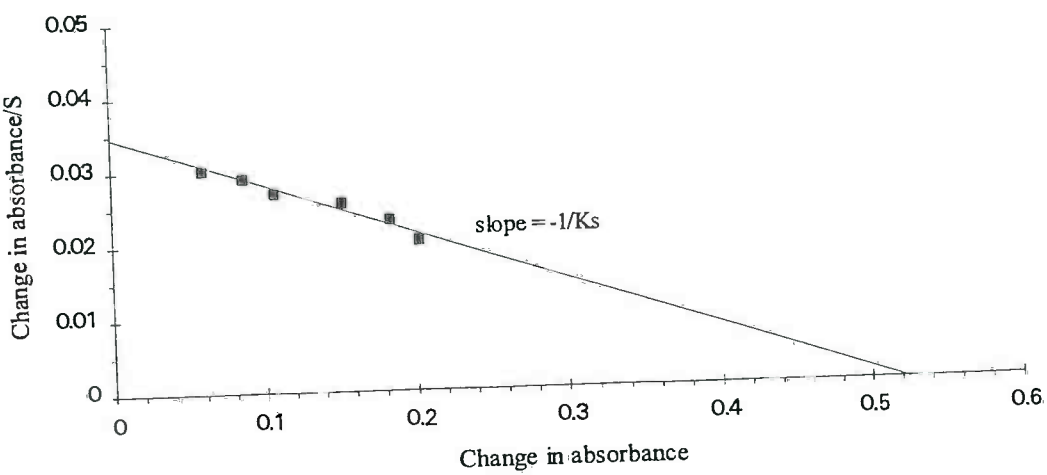

Figure 60 Eadie-Hofstee plot for the binding of benzo(*a*)pyrene with microsomal P450 from *S. cerevisiae*. (S = substrate concentration (µg)).

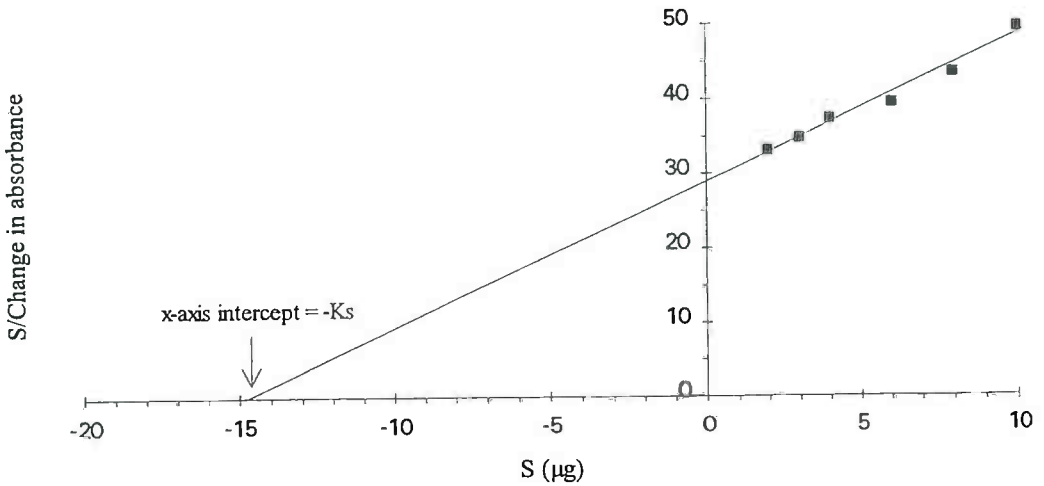

Figure 61 Hanes plot for the binding of benzo(*a*)pyrene with microsomal P450 from *S. cerevisiae*. (S = substrate concentration (µg)).

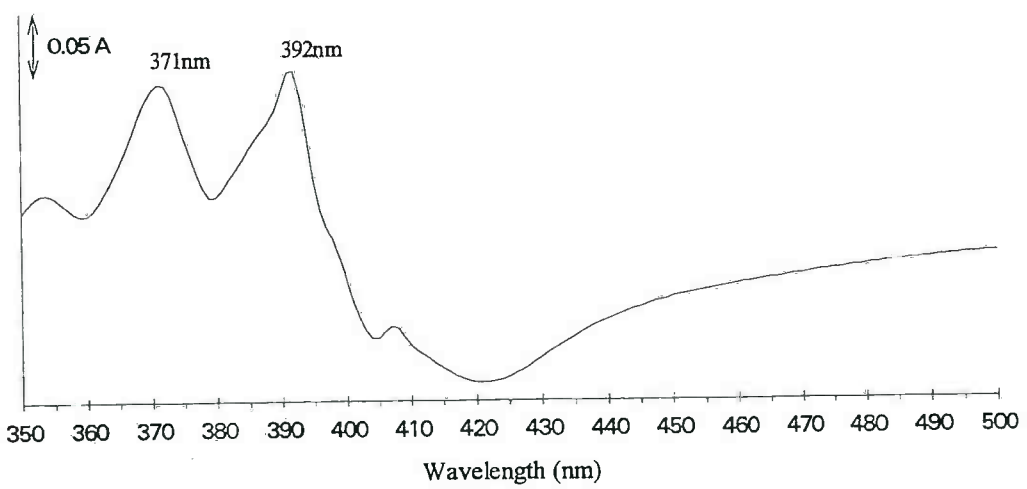

Figure 62 Type I substrate binding on the addition of 10µg/ml benzo(*a*)pyrene to microsomal cyt P450 from *K. marxianus*.

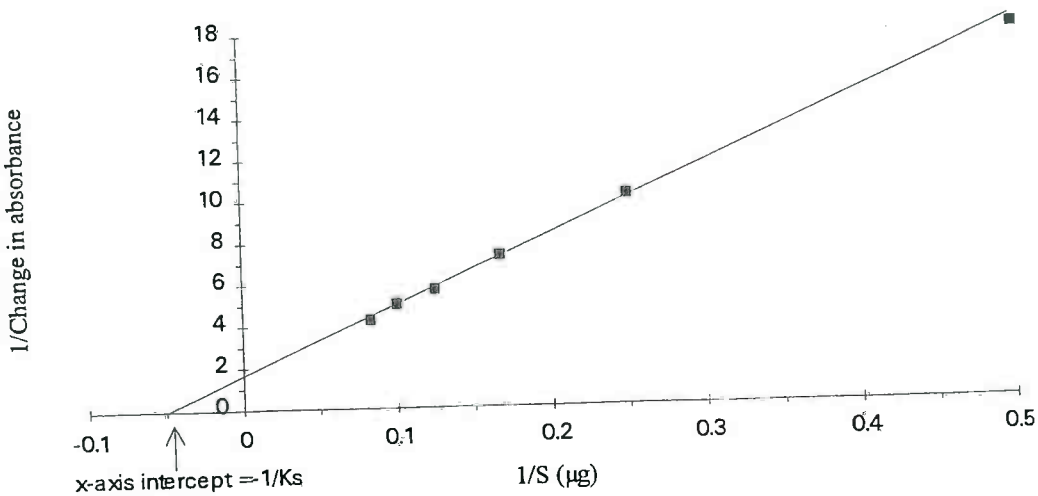

Figure 63 Lineweaver-Burk plot for the binding of benzo(*a*)pyrene with microsomal P450 from *K. marxianus*. (1/S = 1/substrate concentration (µg)).

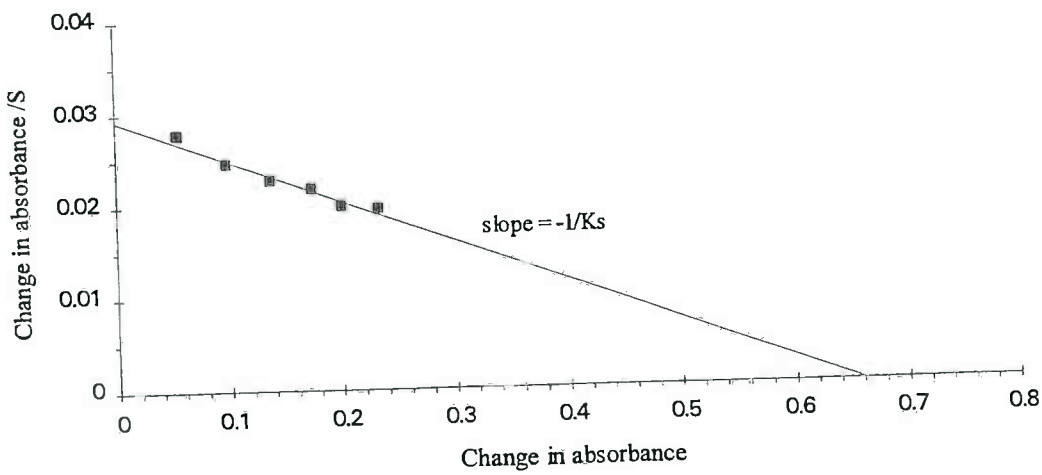

Figure 64 Eadie-Hofstee plot for the binding of benzo(*a*)pyrene with microsomal P450 from *K. marxianus*. (S = substrate concentration (µg)).

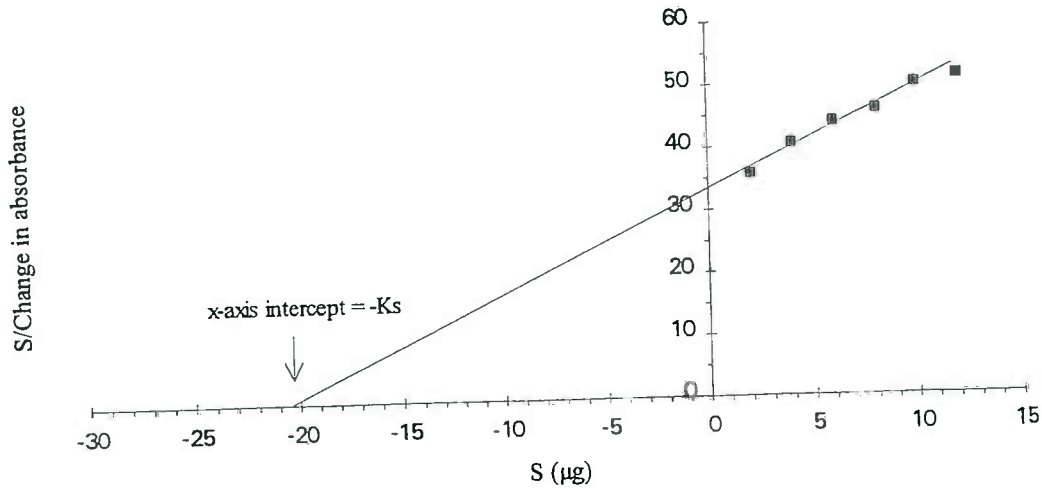

Figure 65 Hanes plot for the binding of benzo(*a*)pyrene with microsomal P450 from *K. marxianus*. (S = substrate concentration (μg)).

Plot type	K_S value (μM)	
	S. cerevisiae	*K. marxianus*
Lineweaver-Burk	68 ± 10	79 ± 11
Eadie-Hofstee	72 ± 15	85 ± 14
Hanes	70 ± 11	82 ± 13
Average K_S	70 ± 12	82 ± 13

Table 53 K_S values for the binding of B(*a*)P to microsomal cyt P450 from *S. cerevisiae and K. marxianus* calculated using various plots (average of two or more experiments).

As Figures 58 & 62 show, the B(*a*)P binding spectra with microsomal samples from *S. cerevisiae* and *K. marxianus* are strikingly similar, and the calculated K_S values are of a similar magnitude (Table 53). These findings contrast sharply with the reduced carbon monoxide difference spectra, which indicate a fairly normal cyt P450 content for microsomal samples from *S. cerevisiae* (Figure 56), but show no detectable cyt P450 for *K. marxianus* (GK1005) (Figure 57). One explanation of this paradox is the masking of the carbon monoxide difference spectrum of *K. marxianus* cyt P450 by other, contaminating haem proteins as discussed above (page 177). Another possibility is that more than one form of cyt P450 is present in yeasts, and that the form responsible for B(*a*)P hydroxylase activity is a minor component in *S. cerevisiae*, and the forms corresponding to the major *S. cerevisiae* component(s) are missing in

K. marxianus (GK1005). Levels of cyt P450 in different yeast strains are known to vary considerably (King *et al.*, 1983b; Karenlampi, 1980) and a cyt P450, other than sterol 14α-demethylase (cyt $P450_{14\text{-}DM}$) which is the predominant cyt P450 in *S. cerevisiae*, was shown to be involved in benzo(*a*)pyrene metabolism in *S. cerevisiae*, strain DK2 (Kelly *et al.*, 1993).

The K_S values for B(*a*)P binding determined in this work are in accordance with literature values. Examples of reported K_S values for the binding of B(*a*)P to microsomal cyt P450 from *S. cerevisiae* (NCYC 754) are 80μM (Bligh, 1988) and 18μM (Azari & Wiseman, 1982); and 50μM for binding to purified cyt P450 (King *et al.*, 1984b).

Although the Lineweaver-Burk modification of the Michalis-Menten equation are classically used calculate K_S values for substrates (Kelly *et al.*, 1985) the distribution of error is non-uniform, and Hanes and Eadie-Hofstee plots, in which the distribution of error is more linear, were also used to determine K_S. In this study, the K_S values obtained using the Hanes and Eadie-Hofstee plots were very similar to those obtained using the Lineweaver-Burk plot, indicating that for these analyses the distribution of error was fairly uniform.

5.2.2.1 Aflatoxin B_1 binding spectra

A spectral change was observed on the addition of aflatoxin B_1 (AFB_1) to microsomal samples from *S. cerevisiae*, resulting in a typical Type I binding spectrum, with a maximum at 391nm and a minimum at 415nm: this is the first report of such a spectrum for AFB_1. A second peak was also observed at 374nm (Figure 66). K_S values were determined from Lineweaver-Burk, Eadie-Hofstee and Hanes plots using equations 10, 11 & 12 (page 100) respectively, and are shown in Figures 67, 68 & 69. K_S values were obtained from each plot and yielded an average K_S value of 178μM (Table 54).

The addition of AFB_1 to microsomal samples from *K. marxianus* did not produce a recognisable binding spectrum (Figure 70). This suggests that, in contrast to the

situation with B(*a*)P, *K. marxianus* (GK1005) lacks a cyt P450 with a suitable substrate specificity for aflatoxins.

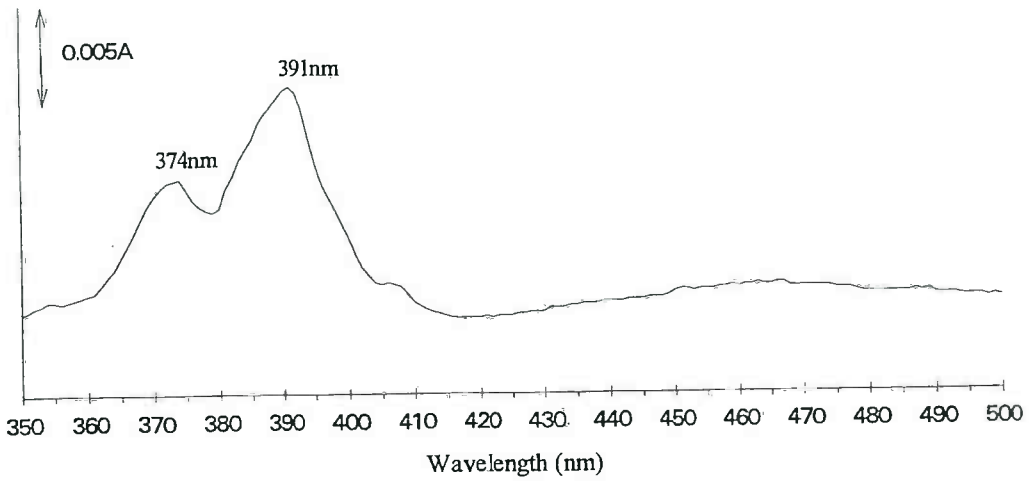

Figure 66 Type I substrate binding on the addition of 5μg/ml aflatoxin B_1 to microsomal cyt P450 from *S. cerevisiae.*

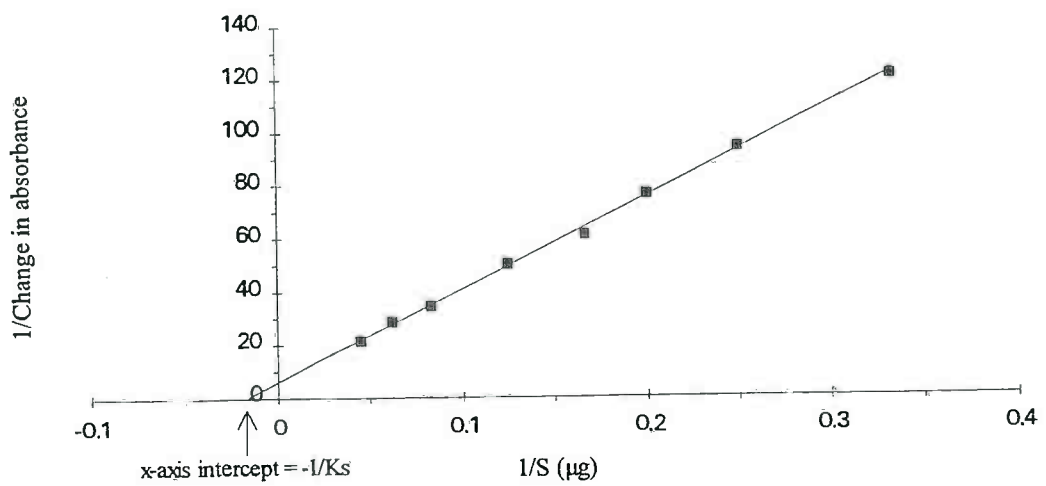

Figure 67 Lineweaver-Burk plot for the binding of aflatoxin B_1 with microsomal cyt P450 from *S. cerevisiae.* (1/S = 1/substrate concentration (μg)).

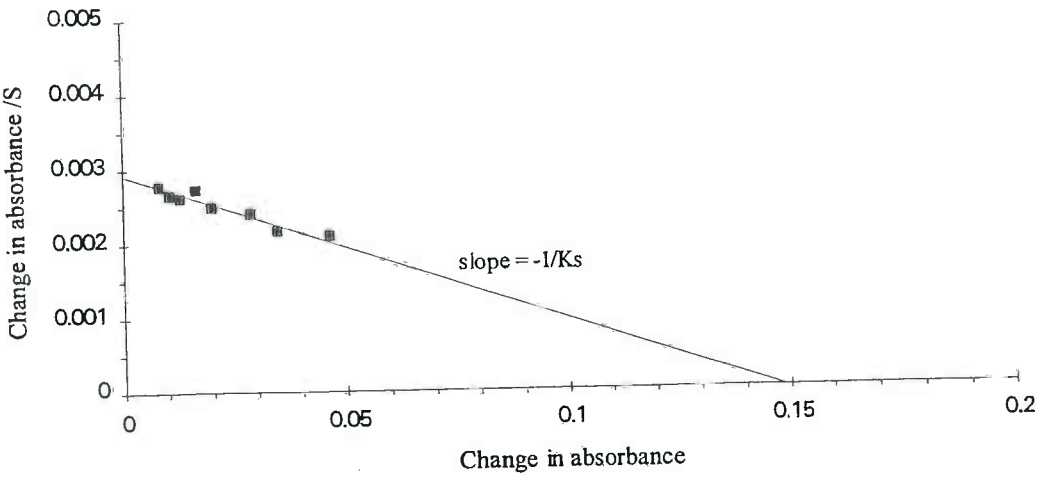

Figure 68 Eadie-Hofstee plot for the binding of aflatoxin B_1 with microsomal cyt P450 from *S. cerevisiae.* (S = substrate concentration (μg)).

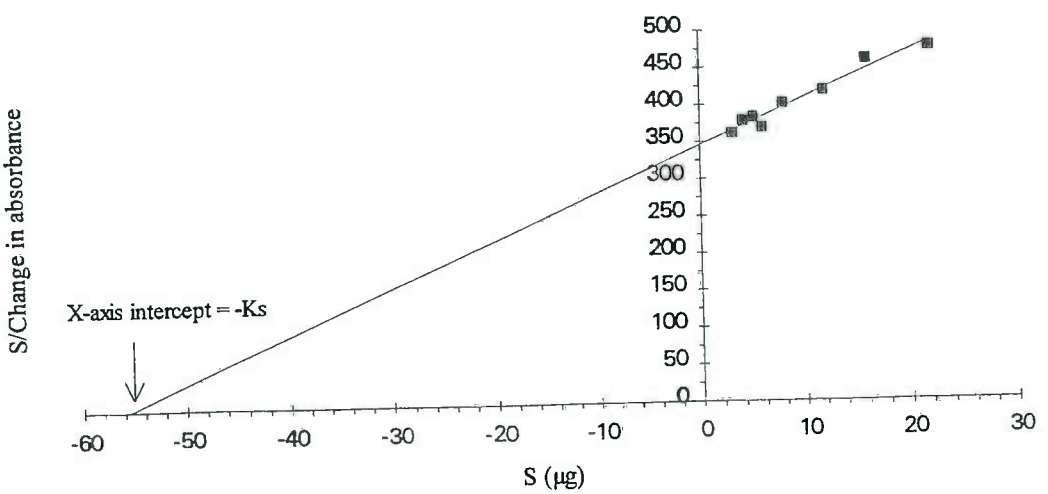

Figure 69 Hanes plot for the binding of aflatoxin B_1 with microsomal cyt P450 from *S. cerevisiae.* (S = substrate concentration (μg)).

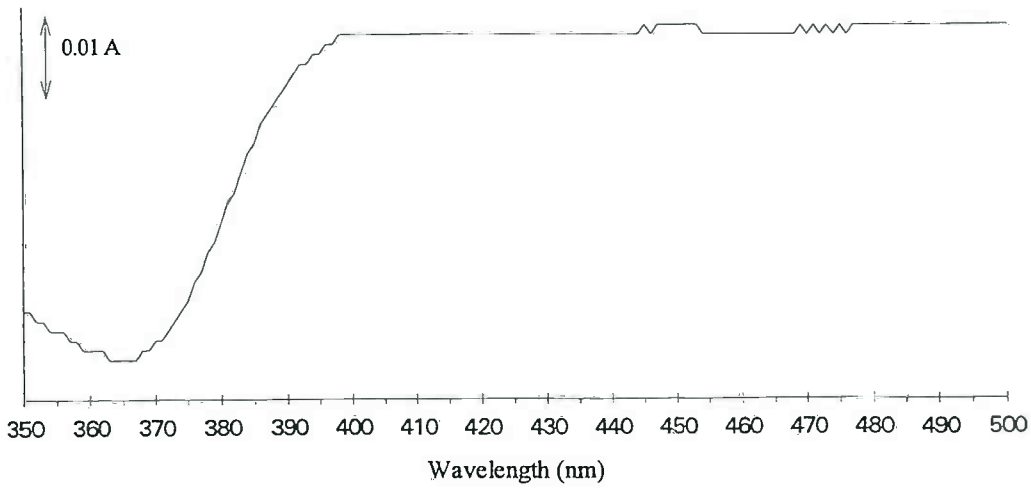

Figure 70 The addition of 10μg/ml aflatoxin B_1 to microsomal P450 from *K. marxianus*- the absence of a binding spectrum.

Plot type	K_S value (μM)	
	S. cerevisiae	*K. marxianus*
Lineweaver-Burke	177 ± 10	No binding
Eadie-Hofstee	172 ± 8	No binding
Hanes	185 ± 7	No binding
Average K_S	178 ± 10	-

Table 54 K_S values for the binding of AFB_1 to microsomal cyt P450 from *S. cerevisiae and K. marxianus* calculated using various plots (average of two or more experiments).

It has been suggested by King *et al.*, (1984b) that the B(*a*)P-metabolising cyt P450 has a narrow substrate range, so presumably, AFB_1 is metabolised by a different form of cyt P450 to that which catalyses the metabolism of B(*a*)P. This second cyt P450 may be a minor form, and is present in *S. cerevisiae,* but lacking in *K. marxianus*.

5.3 CONCLUSIONS

The indication that AFB_1 is not a substrate for cyt 450 of *K. marxianus* (GK1005) may explain to some extent the lack of sensitivity of the yeast bioassay, developed in the work described in this thesis, to aflatoxins. The bioassay was unable to detect AFB_1 and AFM_1 at 25μg/ml. As discussed earlier, aflatoxin toxicity is mediated via cyt P450-dependent epoxidation of the biologically inert parent molecule. The lack of metabolic capability in *K. marxianus* would mean that the aflatoxin would not be metabolised to its toxic metabolite, so explaining the lack of sensitivity to this toxin. In contrast, the cyt P450-dependent metabolism of the trichothecenes results in the production of less toxic metabolites (Swanson & Corley, 1989); in the case of T-2 toxin metabolism results in the production of HT-2 toxin, T-2 triol and T-2 tetraol, which were shown to have decreasing potencies in the structure-activity study. Therefore the lack of ability of *K. marxianus* to metabolise the trichothecenes would mean that the more toxic species (T-2) would persist, rather than being metabolised to a relatively non-toxic derivative. The cyt P450 profile of *K. marxianus* may thus explain the specificity and sensitivity of the *K. marxianus* bioassay to trichothecenes, and the lack of sensitivity of the aflatoxins.

CHAPTER 6.

FINAL CONCLUSIONS AND FUTURE WORK.

A yeast bioassay has been successfully developed for the detection of the trichothecene mycotoxins. Limits of detection vary according to the trichothecene being tested (Table 44, page 146), and range from 0.001μg/ml for verrucarin A to >25 μg/ml for T-2 tetraol.

The assay is based on the inhibition of growth of the yeast *Kluyveromyces marxianus* var. *marxianus* (GK1005), and toxicity can be determined by the spectrophotometric determination of cell density, or by a colorimetric endpoint - the inhibition of β-galactosidase activity, determined by the cleavage of its colorimetric substrate, Xgal.

The addition of 15μg/ml polymyxin B sulphate to the assay medium elicited an increase in the sensitivity of detection (2- to 4-fold), and the use of inhibition of β-galactosidase activity rather than inhibition of growth as the end point for the bioassay produced a further increase in sensitivity (approximately 10-fold). Furthermore, using Xgal as a colorimetric substrate for β-galactosidase allowed the visualisation of toxicity (see Figure 50, page 151) and permitted a qualitative determination of toxicity to be made in the absence of microtitre plate instrumentation. This alongside the speed and technical simplicity of the bioassay allows for its potential use as a field kit - wells containing trichothecene-contaminated samples will remain yellow, whereas wells containing un-contaminated samples will turn blue, following the addition of Xgal.

Using the yeast bioassay, structure-activity relationships between the trichothecene mycotoxins were determined, and the order of toxicity was found to be:

verrucarin A> roridin A> T-2 toxin> diacetoxyscipenol> HT-2 toxin> acetyl T-2 toxin >neosolaniol> fusarenon-X> T-2 triol> scirpentriol> nivalenol> deoxynivalenol> T-2 tetraol.

The most important feature affecting biological activity was found to be the substituent at the R_3 position of the trichothecene nucleus; trichothecenes with a hydroxyl group at R_3 were found to be the least potent, and the presence of an acetyl group enhanced toxicity, but the most potent trichothecenes were those with a macrocyclic side chain

between R_3 and R_4. The potency of the trichothecenes was also modified by changes in other substituents around the trichothecene nucleus, the order of toxicity at R_1 being isovaleryl> hydrogen> hydroxyl and at R_4 acetyl> hydroxyl> hydrogen; by contrast, at the R_5 position, the removal of the acetyl group caused an increase in toxicity.

Although the yeast bioassay, described in this thesis, could be used for the sensitive detection of the trichothecene mycotoxins, it displayed marked insensitivity to other important mycotoxins, including aflatoxins B_1 and M_1 (25μg/ml), and fumonisin B_1, patulin, citrinin, ochrotoxin A, zearalenone, sterigmatocystin, cyclopiazonic acid and tenuazonic acid (10μg/ml); the possible causes of the insensitivity of the bioassay to one of these toxins, AFB_1, were investigated.

Poor penetration of the toxin into the yeast cell is not apparently the major cause of the insensitivity of the yeast bioassay to AFB_1. Studies on the uptake of both T-2 toxin and AFB_1 by *K. marxianus* showed that small, but similar amounts of the two toxins (<0.5% of the total used in each experiment) were recoverable from ruptured cells, yet at the concentrations used, T-2 (10μg/ml) was very toxic causing the complete inhibition of growth whereas AFB_1 (1μg/ml) had no detectable inhibitory effect on growth.

For control purposes the uptake of AFB_1 and T-2 toxin by *B. megaterium* was determined, and the partitioning of recovered toxin was similar to that seen using *K. marxianus*. However, approximately 10% of both toxins was found to be non-recoverable from the *B. megaterium* cultures, whereas recoveries from *K. marxianus* were 100%; this may suggest irreversible binding of the toxin material to the *B. megaterium* cells and is consistent with metabolic alteration/activation of the toxins so they bind firmly to cell structures. Such metabolism may be catalysed by cyt P450; *B. megaterium* is known to contain an active cyt P450 system which may be involved in the metabolism AFB_1 and T-2 toxin. However, as the cyt P450 in *K. marxianus* was not well known, the metabolic capabilities of *K. marxianus* (GK1005) in relation to AFB_1 were investigated.

Results reported here, on the characterisation of cyt P450 in *K. marxianus* (GK1005) suggest that AFB_1 is not a substrate for the cyt P450 of *K. marxianus*. This may explain the lack of sensitivity of *K. marxianus* (GK1005) to AFB_1 and the high level of sensitivity to T-2 toxin and other trichothecene mycotoxins. Aflatoxin toxicity is mediated via cyt P450-dependant epoxidation of the biologically inert parent molecule; the lack of ability of *K. marxianus* to metabolise aflatoxin would mean that the non-toxic parent molecule would persist and the toxic metabolites would not be produced, which could explain the lack of sensitivity of the yeast bioassay to this toxin. In contrast, the cyt P450-dependent metabolism of the trichothecenes results in the production of less toxic metabolites (Swanson & Corley, 1989); in the case of T-2 toxin metabolism results in the production of HT-2 toxin, T-2 triol and T-2 tetraol, which were shown to have decreasing potencies in the structure-activity study. Therefore the lack of ability of *K. marxianus* to metabolise the trichothecenes would mean that the more toxic parent molecule (T-2) would persist, rather than being metabolised to a relatively non-toxic derivative.

The detection of mycotoxins using the yeast bioassay developed in this thesis are in contrast to the findings of a preceding study (Dell, 1993, the findings of which are summarised in Table 20, page 54), in which the same yeast strain (GK1005) was used in a turbidimetric bioassay, using the Bioscreen C tubidimeter (Labsystems), and was able to detect over 60 mycotoxins (including those not detectable using the colorimetric bioassay described in this thesis). One possible hypothesis for the difference in sensitivity of these two assays was the different methanol concentrations used (5% v/v in this study and 8.5% in the Bioscreen assay). However, the presence of methanol was shown not to potentiate the uptake of AFB_1 by *K. marxianus*, and the cause of the enhanced sensitivity of detection of mycotoxins seen in the Bioscreen assay compared to the microtitre plate assay remains unresolved.

Possible lines of future work proceeding from this investigation include:-

- Determination of the limits of detection of the trichothecenes using spiked and naturally-contaminated foods and feedstuffs in the yeast bioassay.
- Determination of the interactive effects of combinations of trichothecenes using the yeast bioassay.
- Further characterisation of cyt P450 in *K. marxianus* (GK1005).
- Determination of the ability of genetically-engineered strains *S. cerevisiae,* expressing specific human cyt P450, to detect mycotoxins.
- Introduction of genes for specific human cyt P450 into *K. marxianus* with the view to enhancing toxicant sensitivity and/or specificity.